

# Quantum Mixtures of Ultracold Atomic Gases

Cosetta Baroni<sup>1,2</sup>, Giacomo Lamporesi<sup>1</sup>, and Matteo Zaccanti<sup>3,4</sup>

<sup>1</sup>Pitaevskii BEC Center, CNR-INO and Dipartimento di Fisica, Università di Trento, 38123 Trento, Italy

<sup>2</sup>Institute for Quantum Optics and Quantum Information (IQOQI), Austrian Academy of Sciences, 6020 Innsbruck, Austria

<sup>3</sup>Istituto Nazionale di Ottica del Consiglio Nazionale delle Ricerche (CNR-INO), 50019 Sesto Fiorentino, Italy

<sup>4</sup>European Laboratory for Non-Linear Spectroscopy (LENS), Università di Firenze, 50019 Sesto Fiorentino, Italy

\*e-mail: cosetta.baroni@ino.cnr.it, giacomo.lamporesi@ino.cnr.it, zaccanti@lens.unifi.it

## ABSTRACT

The combination of different kinds of ultracold gases constitutes a novel powerful experimental framework for the investigation of a variety of physical problems. We illustrate the differences among possible quantum mixtures, be they homonuclear spin mixtures or heteronuclear ones, and show how they can be exploited to investigate a plethora of topics from the few-body to the many-body regimes. In particular, we discuss quantum mixtures of ultracold gases under three different perspectives: systems made of a few atoms of different kinds, single impurities immersed in a host quantum gas, and quantum mixtures of two interacting gases. Given the broad spectrum of possible topics and experimental regimes, in this review we restrict the discussion on single harmonic or flat traps, predominantly in a three-dimensional configuration, suggesting the reader to investigate discrete/lattice physics<sup>1–3</sup> and reduced dimensionality systems<sup>4,5</sup> in other reviews. A selection of results on recent experiments and possible interesting future directions are given.

## Introduction

One hundred years ago Satyendranath Bose<sup>6</sup> and Albert Einstein<sup>7</sup> theoretically predicted that a gas of (then named) bosons can condense in a single quantum state, producing a macroscopic quantum system with long-range coherence and superfluid properties<sup>8</sup>: the so-called Bose-Einstein condensate (BEC). Shortly after, Enrico Fermi<sup>9</sup> and Paul Dirac<sup>10</sup> derived a statistical formalism to describe the behavior of "fermions", particles subjected to the exclusion principle formulated shortly before by Wolfgang Pauli<sup>11</sup>. With these two quantum statistics, we are able to theoretically understand the quantum properties of atomic systems, which can be produced and studied in ultracold atoms laboratories with exquisite control.

Thanks to the rapid advancements in the manipulation techniques of atomic internal and external degrees of freedom with laser cooling, the first BECs were experimentally produced in 1995 at JILA in the group of C. Wieman and E. Cornell<sup>12</sup>, and at MIT in the group of W. Ketterle<sup>13</sup>. In 1999 also the first degenerate Fermi gas was produced at JILA in the group of D. Jin, using similar techniques<sup>14</sup>. Since then, gases of many atomic species have been successfully cooled down to quantum degeneracy, allowing for direct observation of several fundamental quantum phenomena<sup>15–18</sup>.

The improvement in the level of atomic control, also thanks to the observations of Feshbach resonances<sup>19–21</sup>, which allow to tune the interparticle interactions, soon led to the idea of combining atoms of different kinds in such extreme conditions and realize ultracold quantum mixtures. Such systems opened unprecedented possibilities of investigating paradigmatic physics phenomena in diverse research directions, encompassing few- and many-body fundamental problems, such as the realization of ultracold gases of heteronuclear polar molecules<sup>22</sup>, the behavior of impurities in an ultracold gas<sup>23,24</sup>, the exploration of the BCS-BEC crossover in fermionic superfluid mixtures<sup>18</sup>, or the miscible-immiscible phase transition in bosonic superfluid mixtures<sup>25–27</sup>, just to mention a few relevant examples.

This review, targeted to a non-expert reader, aims at introducing the most representative phenomena that can (or could potentially) be explored with such systems, and at providing a brief but comprehensive overview on past and ongoing research on quantum mixtures of ultracold atoms. Owing to the impressive development of this research area and its ramification into several distinct sub-fields, the selection of "relevant" work, and the identification of the "main concepts" regarding quantum mixtures is unavoidably subjective, and partly biased by the specific expertise of the authors<sup>28–30</sup>. In particular, our work mainly focuses on three-dimensional, bulk mixtures of ultracold gases of neutral atoms, although references to research not strictly falling in this category are provided throughout the text. Specifically, we refer the interested reader to extensive reviews, already available in literature, for what concerns the stand-alone but connected areas of quantum mixtures in optical lattices<sup>2,17,31</sup>, of ultracold polar molecules<sup>22,32,33</sup>, and of "hybrid" systems<sup>34,35</sup>, only briefly highlighted in the present article.

Our work is organized as follows: After classifying the various types of quantum mixtures into a few main categories, we provide a general overview of the rich phenomenology associated with such many-body systems. We then discuss in more detail

quantum mixtures from the three viewpoints of few-particle systems, impurity problems, and many-body physics, highlighting, in the final part, future perspectives and possible new directions of this wide research field.

## From homonuclear to heteronuclear mixtures

At least two distinguishable kinds of particles are needed to realize an atomic mixture. Depending on their constituents, it is possible to engineer ultracold mixtures with very different features. Two big categories are represented by *homonuclear (spin) mixtures* and *heteronuclear mixtures*, as illustrated in Fig. 1a. For the sake of simplicity, we will restrict the following discussion to the case of only two components, unless differently explicitly specified.

### Homonuclear spin mixtures

Spin mixtures are homonuclear systems in which all the atoms belong to the same isotope of a given element, but can occupy two different internal "spin" states, depending on the manipulation of their internal degrees of freedom during the preparation and on their dynamical evolution driven by the experimental configuration. The first spin mixture of condensed bosons was realized at JILA with rubidium atoms occupying two different magnetically trappable hyperfine states<sup>36</sup>, shortly after the first BEC. A few years later, mixing together fermions in different spin states successfully led to the achievement of a degenerate Fermi gas without the need for sympathetic cooling techniques<sup>14,37</sup>.

Dealing with a single atomic species, all particles in a spin mixture possess the same mass and quantum statistics. However, they exhibit the fundamental feature of interconversion, i.e., each atom can be prepared in a superposition of the two spin states. On the one hand, this may limit the stability of some spin mixtures that are not immune to exothermal processes – such as spin exchange or dipolar relaxation – that can promote the decay to other unwanted, initially empty states. Experimental tricks relying on the exploitation of quadratic Zeeman effect and light shifts can be used to circumvent this possibility and obtain an effective two-level stable system<sup>38</sup>. Furthermore, it is possible to introduce a coherent coupling between the two states and

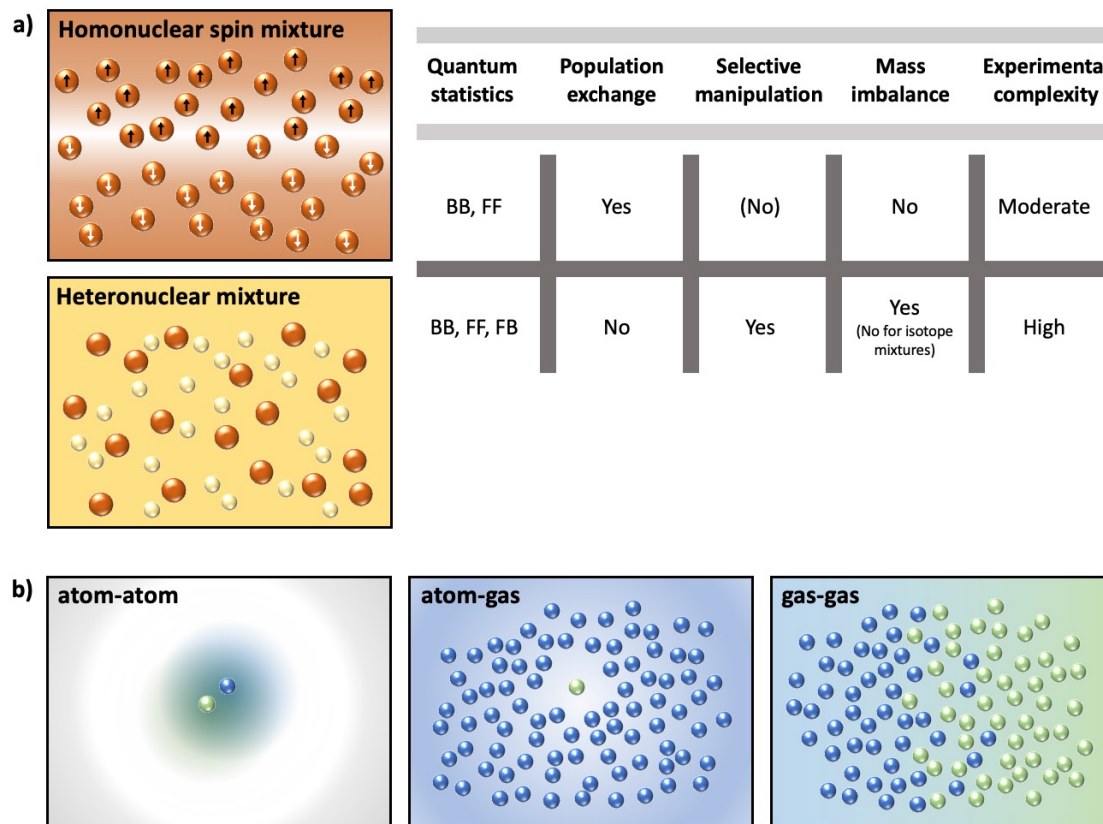


**Figure 1. Different kinds of quantum mixtures.** Schematic representation of quantum mixtures with different constituents. a) Comparison between homonuclear spin mixtures and heteronuclear mixtures. b) Varying the number of atoms involved in each component to investigate physics from few- to many-body problems.

realize systems with intriguing spin dynamics, which permit the quantum simulation of solid-state<sup>39–44</sup> and high-energy<sup>45–47</sup> physics phenomena, and analog gravity<sup>48</sup>.

Typically, the two spin states belong to the electronic ground state, therefore their transition frequency lies in the MHz or GHz range, depending on whether the states are in the same or different hyperfine manifolds. Such a coupling can be introduced using single-photon radiofrequency radiation, which typically results in a uniform field, given the long wavelength with respect to the extension of the atomic samples. Another possibility is using two-photon optical Raman transitions, which provide additionally a local coupling if tightly focused laser beams are used. If the two beams co-propagate, the associated momentum transfer is negligible and the coupling is equivalent to a single-photon microwave transitions. In case of counter-propagating beams, a large momentum transfer is imparted to the atoms, and internal and external degrees of freedom become intertwined, realizing so-called spin-orbit coupled systems<sup>49,50</sup>.

Gases of atoms occupying all the states of a hyperfine level realize a system that shows spinor features<sup>51</sup>. Spinor gases have been experimentally realized in optical traps using sodium<sup>52,53</sup> or rubidium atoms<sup>54,55</sup>, revealing different ground state configurations depending on the intra- and intercomponent interactions. Fermionic spinor gases with more than two components have been studied with ytterbium atoms, realizing strongly correlated systems with tunable SU(N) symmetry<sup>56</sup>.

### Heteronuclear mixtures

Atoms of different species, or different isotopes of a given element, can be cooled down and confined together, realizing an ultracold heteronuclear mixture. Each component of the mixture is characterized by a well-defined atomic mass and statistics, and there is no constraint on the possibility to realize any combination of them. All kinds of statistical mixtures have been realized using different combinations of atomic species, Bose-Bose (BB), Fermi-Fermi (FF), and even Fermi-Bose (FB). While the first two can also be obtained in spin mixtures, the implementation of the latter requires necessarily different atomic species, or at least different isotopes.

The first heteronuclear mixtures of quantum-degenerate gases were realized in 2001 in Florence with a BB combination of <sup>41</sup>K and <sup>87</sup>Rb atoms<sup>57</sup>. In the same year, in Paris, BECs of <sup>7</sup>Li were immersed in a single spin state Fermi sea of <sup>6</sup>Li, forming a quantum-degenerate FB mixture<sup>58,59</sup>. Only in 2008, the first quantum-degenerate two-species FF mixtures were obtained with <sup>6</sup>Li–<sup>40</sup>K in Munich<sup>60</sup> and Innsbruck<sup>61</sup>.

The masses of the constituents can be chosen with ratios that range from approximately one, for instance in the case of isotopic mixtures, to more than 20 for, e.g., Li–Cs<sup>62</sup> and Li–Yb<sup>63</sup>. Systems with a large mass imbalance are ideally suited, for example, to explore Efimov physics thanks to the much smaller ratio between consecutive resonances compared to homonuclear systems<sup>64</sup>, or to study FF mixtures with unmatched Fermi surfaces and asymmetric dispersion relations, leading to exotic types of superfluidity<sup>65,66</sup>. A priori, different species interact in different ways with optical potentials, depending on their own atomic level structure and on the laser wavelength<sup>67</sup>. On the one hand, this represents an experimental complication when one aims at manipulating both species in the same way, but it can also provide a crucial extra degree of freedom for a species-dependent control<sup>68–71</sup>. The schematics in Fig. 1a summarizes the main differences between homo- and heteronuclear mixtures.

Only a few experiments have been reported on mixtures made of three atomic species or isotopes<sup>60,72</sup>.

### From few- to many-body physics

The behavior of quantum mixtures and their ground state configuration depend on many experimental parameters and primarily on the strength of the intercomponent interaction, encoded in the scattering length  $a_{12}$  (unless otherwise specified, we always refer to *s*-wave interactions, being the most relevant ones in the ultracold regime). In order to provide a simple, qualitative picture in which bosonic and fermionic mixtures are compared, let us restrict for simplicity to the case of two gases at zero temperature in a box potential, with equal number of particles ( $N_1 = N_2$ ) and equal masses for the two constituents.

The competition between the intercomponent interaction energy ( $E_{12} \propto a_{12}$ ), which can be tuned experimentally through a Feshbach resonance (FR)<sup>19</sup>, and the energies of the single components ( $E_1, E_2$ ) can give rise to different configurations of the mixture. In order to obtain a unified picture, we can define the dimensionless parameter  $\gamma = E_{12} / \sqrt{E_1 E_2}$  and normalize the total energy of the mixture,  $E$ , as  $\varepsilon = E / \sqrt{E_1 E_2}$ . For the FF case, since there are no interactions between identical fermions due to the Pauli principle, the intracomponent energies are given by the Fermi energies of the single components,  $E_F$ , which are equal in a balanced gas. The Fermi energy introduces a length scale given by the inverse of the Fermi momentum  $k_F = (6\pi^2 n)^{1/3} = \sqrt{2mE_F}/\hbar$ , with  $n$  the density of a single component, so that  $\gamma \sim k_F a_{12}$  and compares the intercomponent scattering length to the mean interparticle distance. For BB mixtures, since intracomponent interactions can be present, we can distinguish between two regimes: When all scattering lengths are small and similar in magnitude,  $\gamma$  reduces to  $a_{12} / \sqrt{a_1 a_2}$ , highlighting the competition between the intra- and intercomponent interactions; otherwise, when the intracomponent scattering lengths are negligible with respect to the intercomponent one, it is convenient to introduce, as for the FF case, an energy scale  $E_n$  connected with the inverse of the interparticle spacing  $k_n = (6\pi^2 n)^{1/3} = \sqrt{2mE_n}/\hbar$ , so that  $\gamma \sim k_n a_{12}$ .

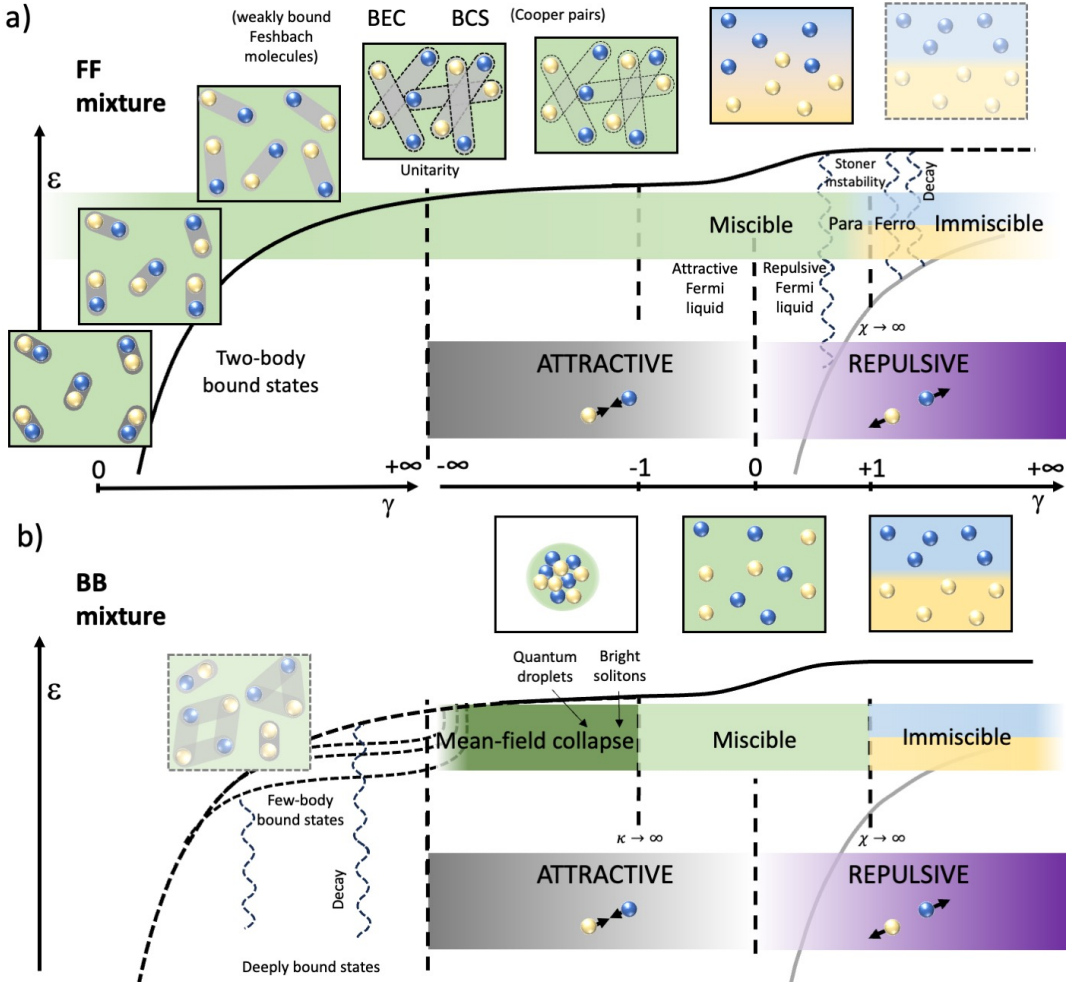


**Figure 2. FF versus BB mixtures.** Different configurations of FF (a) and BB (b) mixtures for different intercomponent interaction strengths and energies. The positive side of  $\gamma$  is reported twice to follow the energy growth both across a FR and across a zero crossing. Dashed lines correspond to unstable configurations.

Figure 2 qualitatively illustrates different possible configurations for FF or BB mixtures as a function of  $\gamma$ . We choose to graphically show the positive region of  $\gamma$  next to the entire  $\gamma$  range from  $-\infty$  to  $+\infty$ , following the growth of the system energy. This representation allows to understand what happens both for large scattering lengths (as for instance near the pole of a FR) and for small ones (when  $a_{12}$  smoothly changes sign across zero). For a given value of  $\gamma$ , more configurations are possible, with corresponding different energies, as the grey line shows on the right side of the diagram.

FF mixtures (Fig. 2a) always occupy the whole available volume, regardless of  $a_{12}$ , because of the Pauli exclusion principle which forbids the spatial overlap of fermions of the same kind. Therefore, if the particle number is fixed, then the density  $n$  is fixed and uniform. On the left side of the diagram, the system ground state is a gas of tightly-bound bosonic molecules, connected with the existence of a two-body bound state, made of two different fermions, which can form also in vacuum, and which features a characteristic size growing for increasing  $\gamma$  (see also next section). As  $\gamma$  becomes very large, the size of individual molecules becomes comparable with the average interparticle distance. The zero-temperature ground state of the system smoothly evolves from a Bose-Einstein condensate of molecules to a Bardeen-Cooper-Schrieffer superfluid of Cooper pairs (BCS-BEC crossover)<sup>18</sup>. On the negative  $\gamma$  side, such many-body pairs at any small but finite temperature lose correlation as  $\gamma$  approaches zero. The FF mixture then smoothly turns from an attractive to a repulsive Fermi liquid as it enters the  $\gamma > 0$  region again, but at a higher energy with respect to the paired ground state. Repulsive FF mixtures are interesting since, similarly to electrons in transition metals, they may undergo a para-to-ferro-magnetic phase transition for  $\gamma \sim 1$ <sup>73-80</sup> – once the intercomponent repulsion overcomes the Fermi pressure – thereby providing a clean framework to explore the textbook Stoner’s model of itinerant ferromagnetism<sup>73</sup>. However, two important features make the physics of repulsive FF mixtures different from

that of ferromagnetic materials in the solid state<sup>81</sup>. First, unlike electrons in metals, where only the total population is fixed, the populations  $N_1$  and  $N_2$  of a FF mixture are generally fixed separately, thus ferromagnetism translates into the formation of spatially-separated domains containing only particles belonging to one or the other component. Second, any repulsive FF atomic mixture represents an excited branch that lays above the energy of the (paired) many-body ground state, into which the system can decay through inelastic recombination processes, which are resonantly enhanced as  $\gamma$  is increased<sup>82,83</sup>: The ferromagnetic instability in ultracold systems thus inherently competes with the pairing one<sup>77,79,80,82-86</sup>.

BB mixtures (Fig. 2b) behave very differently. If the intracomponent interactions are attractive, the corresponding component collapses. The interesting case comes when both gases have repulsive intracomponent interactions, allowing for a stable configuration. Let us start from the right hand side of the plot. For large, positive  $\gamma$ , the intercomponent repulsion dominates over the intracomponent ones and the two gases undergo phase separation occupying different domains in the available volume<sup>87</sup>. The critical value for  $\gamma$  below which the system becomes miscible is  $\gamma = +1$ <sup>52,88</sup>. The BB mixture stays miscible and stable in the range  $-1 < \gamma < +1$ . When  $\gamma$  drops below  $-1$ , attractive interactions dominate and the mixture shrinks occupying a smaller volume than the available one. Within a small range of negative  $\gamma$  the mixture can form bright solitons (in 1D)<sup>89</sup> or quantum droplets<sup>90-92</sup>, and undergo actual collapse and implosion for stronger intercomponent attraction<sup>92-94</sup>. If intercomponent interactions are changed fast enough from repulsive to attractive across the resonant region, the collapse can be overcome and the mixture enters the bound state region forming Feshbach molecules. Since BB mixtures are not subjected to the Pauli exclusion principle, not only two-body bound states of different atoms are possible, but also more exotic few-body clusters, such as Efimov states, may form, that involve more atoms of the same species<sup>64</sup>. Correspondingly, in this regime the system stability is strongly reduced by enhanced loss processes, primarily three-body recombination and inelastic dimer scattering, which drastically limit the lifetime of BB mixtures, even in the non-degenerate regime, at strong interactions  $|\gamma| \gg 1$ . For this reason, producing Feshbach molecules is much more challenging in the BB than in the FF case, and BB dimers are typically created via fast magnetic-field sweeps across the FR, employing dilute, thermal atomic samples<sup>95,96</sup>.

The phenomenology exhibited by FB mixtures, not depicted in Fig. 2, in most cases qualitatively resembles the BB one, both for what concerns the many-body phenomena that can be accessed, and the collisional stability of the system under strongly-interacting conditions<sup>97-101</sup>. A detailed classification of the ground state configurations of such mixtures can be found, for instance, in Ref. 102.

In the following, we enter more in detail and focus on three different regimes: few-body physics, related to problems involving two or three atoms of different kinds in vacuum, the physics of impurities, when single (or a few) atoms of one component are immersed in a bath of particles of a different kind, and many-body physics, studying the interplay and the dynamics of two macroscopic, extended quantum gases.

## Few-atom systems

Fundamental insight on quantum mixtures comes from the characterization of few interacting atoms in vacuum. Before discussing the properties of three-atom systems and higher-order ensembles, it is useful to recall the features of the simplest two-body system of just two particles A + B. We assume that these are confined in a spherical box of radius  $R_{box}$  (although one could employ any kind of trapping potential), and that they mutually interact via a contact-like, short-range potential, fully-characterized by an  $s$ -wave scattering length  $a$  tunable, i.e., via a FR. Figure 3(a) shows the low-energy spectrum associated with (the relative motion of) the two particles<sup>103,104</sup>, plotted as a function of the normalized interaction parameter  $R_{box}/a$ , which plays the same role of  $1/\gamma$  within the many-body scenario of Fig. 2.

Interactions markedly modify the atom-atom spectrum, giving rise to two distinct branches, smoothly connected to the ground-state energy  $E_0 \sim 1/R_{box}^2$  (gray dashed line) of the non-interacting system for  $a=0$ , in strong analogy with the corresponding many-body scenario of Fig. 2. The lowest branch (red line) systematically lays below  $E_0$ , and it thus corresponds to a net A-B attraction. As the resonance pole is approached from the right side, the lowest branch energy monotonically decreases and connects to that of a tightly-bound molecule in vacuum (green short-dashed line) for  $R_{box}/a \gtrsim 1$ . Remarkably, this trend offers a practical way to adiabatically convert ultracold atom pairs into ultracold diatomic molecules, upon sweeping the magnetic field across the FR pole<sup>19,105</sup>. Indeed, ‘magneto-association’ of heteronuclear Feshbach dimers – followed by a coherent optical transfer to their absolute ro-vibrational ground state<sup>106</sup> – currently represents the most efficient method to realize quantum gases of polar molecules<sup>101,107,108</sup>, characterized by a sizable electric dipole moment, and thus by strong, long-ranged interactions. The upper branch (blue line) lays instead systematically above the non-interacting energy, corresponding to a net physical repulsion, which progressively increases across the resonance region, asymptotically approaching the energy of the first excited state of the non-interacting system (marked by the light gray dashed line) as  $a \rightarrow 0^-$ . Interestingly, at the resonance pole  $1/a=0$ , the energy of both branches is independent on  $a$  and scales as  $1/R_{box}^2$  such that the two-body system exhibits a *universal* behavior, in perfect analogy with the many-body case of unitary Fermi gases, see Fig. 2 and next section. As  $R_{box} \rightarrow \infty$ , the above scenario is maintained but the energy spectrum tends to a continuum of scattering states at positive energies, below which a bound molecular level exists for  $a > 0$  at energy  $\epsilon_0 = -\hbar^2/(2m_r a^2)$ , see dashed line in Fig. 3(a). The

energy landscape of Fig. 3(a) holds for any homo- and heteronuclear A-B combination except for two identical fermions, for which *s*-wave scattering is forbidden by the Pauli principle.

The scenario drastically changes when a third particle – say, a second A atom – is added to the system. To gain an intuitive picture of the three-atom problem, let's assume the A majority particles (of mass  $M$ ) to be much heavier than B (of mass  $m \ll M$ ), such that we can treat the system within the Born-Oppenheimer approximation<sup>109</sup>. As for the textbook case of the  $H_2^+$  molecule, one first solves the Schrödinger equation for the light particle in presence of the heavy ones fixed at given A-A distance  $R$ , and then employs the  $R$ -dependent eigenenergies as effective potentials for the heavy particles.

Assuming an intercomponent interaction entirely characterized by a scattering length  $a > 0$  much larger than the Van der Waals range  $l_{VdW}$  such that a weakly-bound dimer exists [dashed line in Fig. 3(a)], for  $R \rightarrow \infty$  the light particle will be localized near either of the two heavy ones. The three-body system thus consists of one AB dimer plus an unpaired A atom and, correspondingly, its energy equals the bare dimer binding energy  $\varepsilon_0$ . For finite distance, instead, the configuration where the B particle is localized near the “left” A atom gets mixed with the one where it is localized near the “right” one. As in the double-well problem with tunneling, the symmetric and antisymmetric superpositions lead to two solutions,  $\varepsilon_+(R)$  and  $\varepsilon_-(R)$ , respectively symmetric and antisymmetric with respect to the permutation of the heavy particles,  $\mathbf{R} \leftrightarrow -\mathbf{R}$ . Figure 3(b) shows the resulting  $\varepsilon_{\pm}(R)$ , normalized to the dimer energy and plotted as a function of the A-A distance  $R$  (in units of  $a$ ). Despite originating from a short-range A-B potential, both  $\varepsilon_{\pm}(R)$  are *long ranged*. The light particle, moving back and forth between the heavy ones, allows particles to feel their mutual interaction over length-scales greatly exceeding  $l_{VdW}$ , and on the order of the scattering length,  $R \sim |a| \gg l_{VdW}$ . In particular,  $V_-(R) \equiv \varepsilon_-(R) - \varepsilon_0 > 0$  corresponds to an effective atom-dimer *repulsion*, which grows for decreasing distance and reaches the three-atom continuum (see shaded gray area in Fig. 3(b)) at  $R = a$ . In contrast,  $V_+(R) \equiv \varepsilon_+(R) - \varepsilon_0$  is a purely *attractive* potential which, for  $R/a \ll 1$ , is found to scale as  $V_+(R) \sim -(\hbar^2 c^2)/(2mR^2)$ , with the dimensionless constant  $c \sim 0.567$ . Depending on whether the heavy particles are identical bosons or fermions, the three-body wavefunction must be overall symmetric or anti-symmetric with respect to their permutation. This implies that for bosonic A atoms  $V_+(R)$  acts on even atom-dimer angular momentum ( $L$ ) channels – in particular on the *s*-wave one. For heavy fermionic particles, instead, the induced attraction occurs in odd channels, and primarily on the  $L = 1$  (*p*-wave) one. Analogously, quantum statistics constrains the  $V_-(R)$  repulsion to odd (even) partial waves for majority bosonic (fermionic) particles. As a result, the effective three-body interactions are long-ranged and multi-channel in nature, although arising from a short-range, *s*-wave direct one.

For the case of majority bosonic atoms – and more generally for any system A-B-C of distinguishable particles with at least two resonant pairwise interactions<sup>64</sup> – the effect of  $V_+(R)$  acting on the lowest partial-wave ( $L = 0$ ) channel leads to the celebrated Efimov scenario<sup>110</sup> (see Refs. 64, 111–114 for extensive reviews), schematically illustrated in Fig. 3(c). Connected with the peculiar  $1/R^2$  scaling of the induced attraction<sup>115</sup> – that for  $1/a = 0$  extends from  $R \sim l_{VdW}$  up to infinite distances, see Fig. 3(b) – the system exhibits an infinite ladder of trimer states  $E^{(n)}$ , characterized by a peculiar “discrete scale invariance”: Starting from the most tightly-bound trimer, at energy  $E_0 \sim \hbar^2/(2ml_{VdW}^2)$  set by the short-range properties of the A-B interaction<sup>64</sup>, Efimov states accumulate towards zero-energy according to a geometric series  $E^{(n+1)}/E^{(n)} = e^{-2\pi/s_0}$ , where the positive dimensionless constant  $s_0$  depends on the specific system considered, in particular upon the mass ratio  $M/m$ <sup>64</sup>. Moving out of resonance, the energy of each trimer (red lines in Fig. 3(c)) is modified in a surprising fashion: For  $a < 0$ , where no dimer exists, the  $n$ -th Efimov trimer persists, within a kind of “Borromean binding”, up to a critical value  $a_*^{(n)} < 0$  (see black dots in Fig. 3(c)) where it hits the three-atom continuum. Moving towards small  $a > 0$  values, while the AB dimer becomes increasingly more bound (black line), the trimer energies progressively approach the dimer one, hitting it at specific  $a_*^{(n)} > 0$  values (see empty gray circles). Similarly to the  $E^{(n)}$  energy spectrum at resonance, both series of  $a_-^{(n)}$  and  $a_*^{(n)}$  feature the peculiar discrete scale invariance  $a_-^{(n+1)}/a_-^{(n)} = e^{\pi/s_0}$ . An important consequence of the induced  $1/R^2$  attraction characterizing the Efimov's scenario is that it inherently favors the three atoms to approach each other at short distances,  $R \sim l_{VdW}$ . This favours inelastic loss processes – such as three-body recombination or inelastic atom-dimer scattering towards deeply-bound molecular levels – that are enhanced as the resonant regime, or an Efimov resonance, is approached, limiting the lifetime of  $N > 3$  boson systems at strong interactions<sup>116,117</sup>. Efimov's prediction<sup>110</sup>, dating back 1970, has been successfully explored since 2006<sup>118</sup> in different homo- and hetero-nuclear systems<sup>64</sup>. Particularly relevant for the topic of this review is the exploration of the Efimov scenario in three-component spin mixtures of ultracold  $^6\text{Li}$  atoms<sup>119–123</sup>, in  $^{41}\text{K}$ – $^{87}\text{Rb}$  Bose-Bose<sup>124</sup> and  $^{40}\text{K}$ – $^{87}\text{Rb}$  Fermi-Bose<sup>125</sup> mixtures and, more recently, also in the two extremely mass-imbalanced Fermi-Bose combinations  $^6\text{Li}$ – $^{133}\text{Cs}$ <sup>126,127</sup> and  $^6\text{Li}$ – $^{87}\text{Rb}$ <sup>128</sup>. In particular, the latter two systems are significantly more advantageous than homonuclear ones to reveal the presence of few-body clusters, and to test their discrete scale invariance. This can be understood by considering that for  $M/m \gg 1$ , within the Born-Oppenheimer approximation,  $s_0 \propto \sqrt{M/m}$ , implying that the larger the  $M/m$  ratio, the smaller the scaling factor  $e^{\pi/s_0}$ , and thus the denser the Efimov spectrum will be<sup>64</sup>. Correspondingly, the chance to find, within realistically-accessible ranges of scattering lengths below the unitary limit<sup>116,117</sup>, multiple  $a_-^{(n)}$  and  $a_*^{(n)}$  resonances is significantly enhanced for highly-imbalanced mixtures, with respect to the equal-mass case. For instance, exact calculations (see Ref. 64 for details)

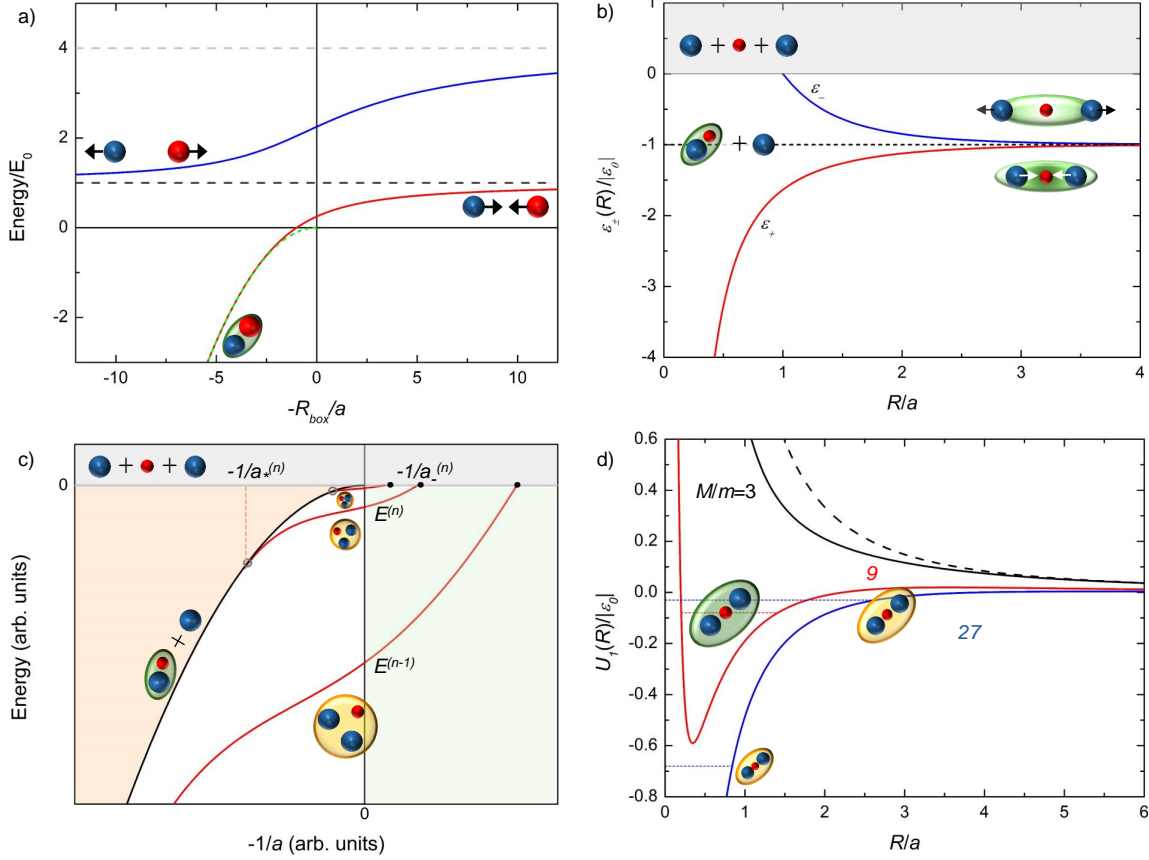


**Figure 3. The few-atom problem.** (a) Low-energy spectrum of two interacting atoms in a spherical box. (b) Born-Oppenheimer potentials as a function of the distance between the two heavy particles. (c) Sketch of the Efimov scenario. (d) Total Born-Oppenheimer potential  $U_1(R)$  for two heavy fermions plus a third atom as a function of the  $M - M$  distance and different  $M/m$  values, see legend. Dashed line denotes  $V_{cb}(R)$  for  $M/m = 3$ .

foresee for  $M_{Cs}/m_{Li} \sim 22.1$  a scaling constant  $e^{\pi/s_0} \sim 4.88$ , significantly smaller than the one holding for three identical bosons, of about 22.7. This has allowed for the observation of up to three consecutive Efimov resonances in Li-Cs mixtures<sup>127</sup>, whose relative location quantitatively confirmed the theory predictions.

When majority fermions, rather than bosons, are considered, the scenario qualitatively changes. On the one hand, the fact that the lowest  $s$ -wave channel of the three-atom system is associated with the  $V_-(R)$  repulsion prevents atoms to approach at short distances, making resonantly-interacting FF mixtures much more stable than those involving (at least one) bosonic species, e.g. enabling the realization of the unitary Fermi gas and the study of crossover superfluidity<sup>18</sup>. On the other hand, the induced attraction  $V_+(R) \propto -1/(mR^2)$  occurs in the  $p$ -wave channel, where it competes with the effective repulsion set by the centrifugal barrier  $V_{cb}(R) \propto +1/(MR^2)$ . This results in an overall potential  $U_1(R) = V_+(R) + V_{cb}(R)$  which, as illustrated in Fig. 3(d), strongly depends upon the system mass ratio at the qualitative level, contrarily to the previously discussed bosonic case. For  $M/m \geq 13.6$  (see e.g. blue line for  $M/m=27$ )  $V_+(R)$  dominates over  $V_{cb}(R)$  at all distances, leading to the Efimov scenario (see Fig. 3(c)), although here trimers carry a non-zero angular momentum. As the mass ratio is progressively lowered below such a critical value, the centrifugal barrier overcomes the induced attraction at short distances, and  $U_1(R)$  first develops a shallow minimum at large inter-particle distance  $R \sim a$  (see red line), that then disappears until  $U_1(R)$  asymptotically approaches the centrifugal barrier for small mass ratios (see e.g. dashed versus solid black line in Fig. 3(d)). Yet, for intermediate mass ratios  $8.17 \leq M/m \leq 13.6$ , the potential well in  $U_1(R)$  is deep enough to support (at most two) bound states<sup>129</sup>. Such Kartavtsev-Malykh (KM) trimers starkly differ from Efimov ones: Like Feshbach dimers, they are loosely-bound cluster states that exist only for  $a > 0$  and exhibit universal properties, solely determined by the scattering length and the mass ratio  $M/m$ , as long as finite-range corrections are negligible<sup>130</sup>. Moreover, KM trimers (and higher-order non-Efimovian clusters) are expected to be collisionally stable – since the potential barrier prevents particles to approach each other at short distances, see red line in Fig. 3(d). This makes them appealing also at the many-body level, where they are predicted to promote qualitatively new regimes of strongly-correlated fermionic matter<sup>131, 132</sup> beyond the equal-mass scenario of Fig. 2(a). Such few-body states

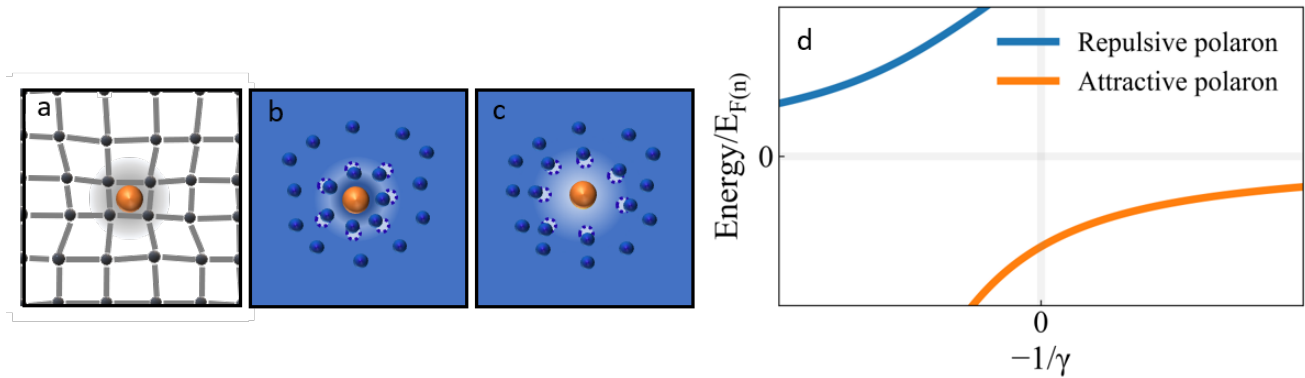


**Figure 4. Polaron.** Pictorial representation of a polaron in solid state (a) and its counterpart in quantum gases in the attractive (b) and repulsive (c) cases. d) Energy spectrum showing the repulsive and attractive polaron branches (numerical data for a homonuclear spin mixture, courtesy of P. Massignan).

lack experimental observation thus far, although the strong  $p$ -wave atom-dimer attraction revealed in  ${}^6\text{Li}$ - ${}^{40}\text{K}$  mixtures<sup>133</sup> is a precursor of a KM trimer at sub-critical  $M_K/m_{\text{Li}} \sim 6.6$  value. In the future, stable KM trimers may be accessible with newly-realized  ${}^6\text{Li}$ - ${}^{53}\text{Cr}$  Fermi mixtures<sup>134-136</sup> ( $M_{\text{Cr}}/m_{\text{Li}} \sim 8.8$ ) and other FF systems of smaller mass ratio<sup>137, 138</sup>, but confined in low dimensions (2D, 1D), where the centrifugal barrier is weakened, thereby favoring cluster formation at lower  $M/m$  values, see e.g. <sup>139, 140</sup>. Finally, we remark that a variety of few-body cluster states with  $N > 3$  have been also considered and partly explored<sup>64</sup>. Quite generally, for majority-boson systems one expects that binding of arbitrarily large clusters is allowed by the  $1/R^2$  shape of the induced attraction. Although calculations become increasingly difficult with larger number size, this trend has been experimentally-confirmed at least for 4-body Efimovian states<sup>141</sup>. In contrast, binding arbitrarily large numbers of fermions is ruled out beyond five-body clusters, owing to the  $p$ -wave symmetry of the channel supporting the induced attraction<sup>142</sup>.

### Atom-gas (impurity problem)

By increasing the number of scattering partners that a particle can have, we enter the many-body regime<sup>143</sup> and it is convenient to think at such system as an impurity B atom embedded into a continuous, host bath formed by the majority A particles. Understanding this extremely-polarized regime is relevant since the impurity limit exhibits some of the critical points of the full zero-temperature phase diagram<sup>144</sup>. For weak interactions, the energy of a single impurity is modified with respect to the non-interacting value by the mean-field energy, which is negative for  $a_{12} < 0$  and positive for  $a_{12} > 0$ . Analogously, the energy of the  $n$ -mer is shifted by the mean-field effect. The resulting states are the analytic continuation of the vacuum ones described in the previous section (see Fig. 3a). For strong interaction, the impurities will create excitations in the bath, in the form of Bogoliubov modes or particle-hole fluctuations in a Bose condensed or in a degenerate Fermi bath, respectively, which markedly modify the impurity properties, relative to the bare ones in vacuum. In this context, it is convenient to describe the system in terms of *quasiparticles* following the concepts originally introduced by Landau, Pekar<sup>145</sup>, and Fröhlich<sup>146</sup>. In this framework, an electron moving through a ionic crystal can be conveniently described as a quasiparticle, formed by the bare electron dressed by the polarization cloud induced by its interaction with the lattice ions (see Fig. 4a). Similarly, the complicated many-body system, realized by letting few impurity atoms strongly interact with a (Fermi or Bose) gas, can be mapped into a weakly-interacting liquid of quasiparticles, made by the bare impurities dressed by excitations of the host bath, with renormalized properties, such as energy and effective mass. In this picture, the overlap between the quasiparticle and the bare particle is encoded in the so-called *quasiparticle residue*<sup>81</sup>. The literature refers to these quasiparticles as *polaron*, *dimerons*, *trimerons*, etc., when arising from the dressing of a single B impurity, a A-B molecule, a A-A-B trimer, and so on<sup>147</sup>. In particular, the dressed state connected to the atomic impurity attractively (repulsively) interacting with the host gas is referred to as the attractive (repulsive) polaron (see Fig. 4b and c). Note that the dimeron, also referred to as *dressed molecule* or *molaron*, should not be confused with the bare *Feshbach molecule* (see green line in Fig. 3a): Like for the polaron case, its energy is strongly modified by the surrounding medium and, as discussed below, it may, or may not, represent the system ground state.

## Fermi and Bose polarons

While the statistics of the single impurity is irrelevant, the one of the bath defines the polaron properties, and we distinguish between Bose and Fermi polarons, depending whether the bath is formed by a degenerate Bose or Fermi gas, respectively. The Bose polaron is analogous to polarons created in solid state systems described by the Fröhlich Hamiltonian<sup>148</sup>, whereas the Fermi polaron is a prototypical realization of the fundamental building block of a Landau's Fermi liquid<sup>81</sup>.

In Fig. 4d the energy landscape of the impurity-bath system is sketched as a function of the intercomponent interaction. Contrarily to the two-body system of Fig. 3a, here three rather than two distinct spectral features are identified: one corresponding to the attractive polaron (orange line), one to the metastable repulsive polaron (blue line)<sup>149</sup> and a third dimeronic one, not shown, asymptotically connected, for vanishing bath density, to the bare Feshbach molecule presented in Fig.3a. While this scenario qualitatively holds for both bosonic and fermionic media, some caveats are necessary. First of all, in the case of a bosonic bath, the dimeron energy asymptotically approaches the attractive polaron branch from above while never crossing it, such that the attractive polaron is the system ground state at all interaction strengths.

In the case of a fermionic bath, instead, the two branches intersect at the so-called *polaron-to-molecule transition* where the ground state changes from the attractive polaron to the dimeron.

Experimentally, it has been observed that this crossing point is smoothed by increasing impurity concentration and temperature<sup>150</sup>. Secondly, the stability of the bath plays a crucial role in determining the quasiparticles lifetime. Thanks to the Pauli exclusion principle, the Fermi bath is stable against  $n$ -body losses at all interaction strengths and, therefore, attractive polarons (and dimers) are found to persist over timescales exceeding by several orders of magnitude the typical Fermi time of the host gas<sup>23</sup>. In contrast, enhanced inelastic processes that affect bosonic media in the resonant regime (see previous section), strongly reduce the quasiparticles lifetime, relative to their fermionic counterparts. In the Fermi case<sup>23,151</sup> the impurity properties under resonantly-interacting conditions appear to share universal behavior, solely controlled by the bath density – hence by  $E_F$  – in strong analogy with both the two-particle system (see Fig. 3a and related discussion) and the unitary Fermi gas case<sup>18</sup>, realized with balanced FF mixtures, see next section. In the Bose case, instead, due to three-body correlations, the Bose polaron is generally not scale invariant at unitarity, but depends on an additional Efimov length scale<sup>152</sup>. Nonetheless, some universal behaviors have been observed in experimental works on Bose polarons<sup>153,154</sup>.

Introduction of a mass asymmetry between the impurity atom and the particles of the host gas can qualitatively change the impurity problem. In particular, light impurities are expected to promote the emergence of novel types of quasiparticles within fermionic media<sup>155,156</sup>, linked to the existence of higher-order clusters at the few-body level discussed in the previous section. Similarly, light impurities in a Bose gas are sizably affected by increased three-body correlations even at weak coupling and, for stronger intercomponent attraction, the atom-like polaronic state is predicted to smoothly cross-over to a (dressed) Efimov trimer<sup>152,157</sup>. In the opposite limit of an infinitely massive impurity, in a fermionic bath the interacting many-body system is predicted to completely lose any overlap with the non interacting one<sup>158,159</sup>, leading to the so-called Anderson orthogonality catastrophe<sup>160</sup>. An analogue effect is predicted also for impurities in a non-interacting Bose gas, for both infinite and finite impurity mass<sup>161</sup>.

Standard experimental techniques to investigate polaronic systems are provided by spectroscopic methods<sup>162</sup>. The energy landscape is routinely accessible via radio-frequency spectroscopy, which led to the first observation of the attractive Fermi polaron in an ultracold  $^6\text{Li}$  FF spin mixture<sup>23</sup>. The full polaron spectrum was recorded for the first time in a FF heteronuclear mixture of  $^6\text{Li}$  and  $^{40}\text{K}$ <sup>163</sup>, observed then also in a  $^6\text{Li}$  FF<sup>86</sup> and in a  $^6\text{Li}$ – $^{41}\text{K}$  FB mixture<sup>164</sup>. The Bose polaron spectrum was recorded for the first time in parallel in a heteronuclear mixture of  $^{87}\text{Rb}$ – $^{40}\text{K}$ <sup>165</sup> and a spin mixture of  $^{39}\text{K}$ <sup>166</sup>. The out of equilibrium formation dynamics of the polaron has been investigated via Ramsey interferometric techniques for both the Fermi<sup>167</sup> and the Bose<sup>168</sup> polaron. While other polaronic quantities can be inferred from radio-frequency spectroscopy, such as the effective mass<sup>86</sup> and the polaron residue<sup>23</sup>, there are more suitable tools, such as Rabi oscillations<sup>86,163,169</sup>, transport measurements<sup>151,170</sup>, Raman<sup>150</sup> and momentum-resolved photoemission<sup>171</sup> spectroscopy.

By increasing the number of impurities, interactions between the corresponding polarons, mediated by modulations of the bath, appear. While the quantum statistics of the impurity is irrelevant in the single impurity limit, it is crucial for a finite impurity concentration: In particular the mediated interactions between polarons are always attractive or always repulsive for bosonic or fermionic impurities, respectively, regardless the sign of the interaction between the impurities and the bath<sup>172</sup>. Such interactions were experimentally observed for polarons formed by both bosonic and fermionic impurities in a Fermi sea in Ref.<sup>173</sup>. Additionally, due to the attractive nature of the effective interaction between two polarons formed by bosonic impurities, the formation of bound states of two polarons, named *bipolarons*, has been theoretically predicted<sup>174</sup> but not yet experimentally observed.

We conclude this section remarking that nowadays the investigation of the impurity problem<sup>175</sup> is, on the one hand, not only restricted to 3D systems, but extends also to reduced dimensionality, such as 2D<sup>171</sup> and 1D<sup>176–178</sup>, on the other hand, not only restricted to neutral mixtures with contact interactions, but also encompasses charged impurities<sup>179,180</sup> or Rydberg atoms<sup>181</sup>.

## gas-gas (many-body physics)

Since FF and BB mixtures are usually investigated in different interaction regimes and the physics of the many-body system strongly depends on the quantum statistics of the constituents, here we treat the two types of mixtures separately. For a general overview of many-body physics investigated with ultracold atoms, considering also lattices and lower dimensionality, we refer the reader to Ref.<sup>2,17</sup>.

### Fermi-Fermi

Let us now consider a mixture of fermions with equal population and equal masses, such as the homonuclear spin mixture sketched in Fig.2. Because of Pauli blocking there are no intracomponent interactions and the main interest in such mixtures arose from the possibility to investigate a strongly interacting gas without being affected by strong losses, contrary to the BB case. In particular, thanks to Feshbach resonances, the intercomponent interactions can be tuned from repulsive to attractive, crossing the pole of the resonance, where scattering length  $a_{12}$  diverges and the system exhibits *universal* features<sup>182</sup>.

The behavior of a balanced attractive Fermi-Fermi mixture across a Feshbach resonance is captured by the so-called BEC-BCS crossover<sup>18</sup>, the phase diagram of which is reported in Fig. 5. As already pointed out in the discussion of the few-body physics, for positive scattering lengths  $a_{12}$  there exists a bound state, which is more bounded the smaller the scattering length. If now we consider a macroscopic number of atoms we have a large number of such molecules which, being created by bounding two fermions, are bosonic in nature and so can undergo Bose-Einstein condensation for temperatures below the critical temperature  $T_c$ , of the order of fractions of the Fermi temperature  $T_F$ : The mixture behaves as a superfluid of a single bosonic component. We refer to this interaction regime as the BEC side of the resonance. Condensed molecules in this regime have been first observed in homonuclear mixtures of <sup>6</sup>Li<sup>183,184</sup> and <sup>40</sup>K<sup>185,186</sup>.

For negative scattering lengths, instead, two atoms can form a large pair with total momentum equal to zero, in analogy with the Cooper pairs of electrons predicted by the BCS theory of superconductivity<sup>187</sup>, and we identify this side of the resonance as the BCS side. The fact that the Cooper pairs have zero momentum arises from the fact that for equal populations and equal masses the Fermi surfaces relative to the two components are equal. One can see that pairing of atoms with opposite momentum is favored because of their higher density of states leading to a higher binding energy with respect to pairs formed with not zero momentum<sup>188</sup>. If there is instead a population or a mass imbalance in the mixture, the two Fermi surfaces do not match anymore and the system, as we shall see, has to find a way to compensate this mismatch. Contrary to the molecular states on the BEC side, the Cooper pairs do not exist in vacuum and are the result of the many-body nature of the gas. Indeed, in a Fermi sea, because of Pauli blocking, we can describe the system considering only atoms whose momentum lies on top of the Fermi surface, making the gas an effectively 2D system, for which a loosely bound state exists for infinitesimally small attraction. These pairs can also condense for low enough temperature, but now the critical temperature scales exponentially with the inverse of the scattering length, as can be seen in the phase diagram in Fig. 5. Observation of Cooper pairing in momentum space has been recently observed in a mesoscopic two-dimensional Fermi-Fermi mixture<sup>189</sup>. For scattering lengths close to the pole of the Feshbach resonance, there is a crossover between a superfluid of condensed molecules and one of condensed Cooper pairs, where the pair is not as bounded as a molecule and not as loose as a Cooper pair. Condensation of such pairs was first observed in Ref.<sup>190</sup> and the superfluid nature of the gas across the resonance was investigated in<sup>191–194</sup>. A review of early experimental achievements in the BEC-BCS crossover can be found in Ref.<sup>195</sup>.

Let's consider now an unbalanced mixture and let's start with the case of population imbalance and equal masses, for simplicity. As we saw until now, in the case of a balance mixture we can have a superfluid formed by pairing all the atoms composing the gas, in the limit of one single impurity in the Fermi sea of a majority of atoms, a polaron is formed. There should be then a phase transition between these two states, connecting the superfluid to the normal Fermi gas<sup>197</sup>. In particular, superfluidity breaks down at the so-called Chandrasekhar–Clogston limit<sup>198,199</sup>, where the difference between the two Fermi energies, arising from the population imbalance, is larger than the energy gained in creating a pair. Experimentally, the critical population imbalance for which superfluidity is lost has been investigated in Refs.<sup>200–202</sup>.

Superfluidity in an imbalanced Fermi gas can appear in different ways, depending on how the system compensates the mismatch in the Fermi energies of the two components. For detailed reviews on imbalanced Fermi gases, we refer the reader to Refs.<sup>65,203</sup>

In the simplest scenario condensed pairs are created, which phase-separate with the remaining unpaired atoms, resulting in two spatially separated phases given by a superfluid and a normal polarized Fermi gas, as observed in Ref.<sup>200</sup>.

More exotic superfluid phases are predicted<sup>65</sup>, even though not yet experimentally observed. Two main scenarios are possible: if pairing occurs between particles at the surface of their respective Fermi seas, the pairs acquire a momentum equal to the difference of the two Fermi momenta, and which can be interpreted as a spatial modulation of the order parameter. This is named Fulde–Ferrell–Larkin–Ovchinnikov (FFLO) phase<sup>204–206</sup>. Another possibility is to form pairs at zero momentum at the cost of opening a gap inside the Fermi sea of the majority component, Sarma phase<sup>207,208</sup>.

It is theoretically predicted that adding mass imbalance to a system would rise the critical temperature for these exotic pairings, favoring the elusive experimental observation of such states<sup>66,209</sup>. Nowadays available mass imbalanced FF mixtures

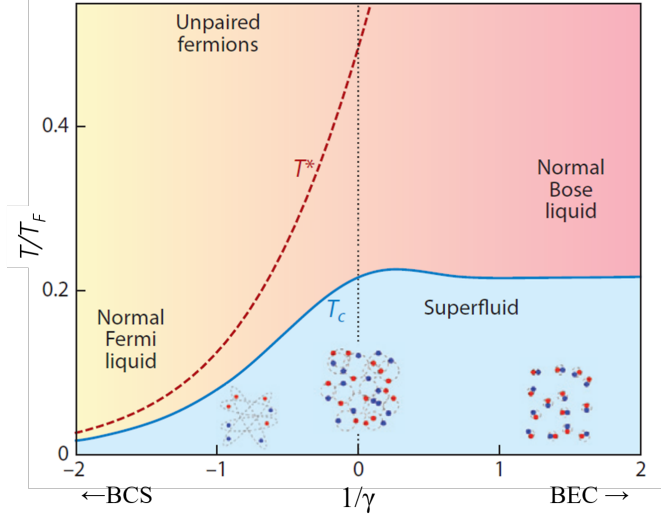


**Figure 5.** Phase diagram of the balanced mixture. The red-dotted and blue continuous lines indicate the temperatures below which the pairs are formed,  $T^*$ , and condensed,  $T_c$ , respectively. Adapted from<sup>196</sup>.

are  $^6\text{Li}-^{40}\text{K}$ <sup>28,210</sup>,  $^{161}\text{Dy}-^{40}\text{K}$ <sup>28</sup>,  $^6\text{Li}-^{173}\text{Yb}$ <sup>63,211</sup>,  $^6\text{Li}-^{53}\text{Cr}$ <sup>134,136</sup>, and  $^6\text{Li}-^{167}\text{Er}$ <sup>212</sup>.

As anticipated in the previous sections, also repulsive FF mixtures have attracted a growing interest that, for bulk systems subject of this work, mainly connects to the possible exploration of the textbook Stoner's model for itinerant ferromagnetism<sup>73–76</sup>, see Ref.<sup>81</sup> for an extensive review. This owes to the fact that such ultracold systems embody the two ingredients of Stoner's Hamiltonian<sup>73</sup> – Fermi pressure and short-range repulsion – free from intricate band structures, additional kinds of interactions, and disorder inherent to any condensed matter system. However, experimental attempts in this direction revealed a much richer and more subtle behavior, very different from the original Stoner scenario.

Although convincing signatures for a ferromagnetic instability within the repulsive Fermi liquid have been obtained, through studies of spin dynamics of a FF mixture prepared in an artificial magnetic domain-wall structure<sup>78</sup>, and via time-resolved quasi-particle spectroscopy both on balanced<sup>79</sup> and imbalanced<sup>86</sup> mixtures, already early experiments<sup>77,85</sup> found the system dynamics to be fundamentally affected by another type of instability, antithetical to ferromagnetism, and associated with the tendency of repulsive fermions to combine into weakly bound pairs. This latter mechanism is intimately linked to the short-ranged nature of the interatomic interaction: The strong repulsion,  $\gamma \sim 1$  (see Fig. 2(a)), necessary for ferromagnetism to develop<sup>73–76</sup> can only be attained if a weakly bound molecular state exists below the two-atom scattering threshold, see Fig. 3(a). As such, the repulsive Fermi gas represents an excited metastable branch of the many-body system, inherently affected by decay processes towards lower-lying molecular states, which become faster for larger repulsive interactions<sup>82–85</sup>. Pump-probe spectroscopic studies<sup>79</sup> provided measurements of the rates at which pairing and short-range ferromagnetic correlations develop after creating a strongly repulsive Fermi liquid, finding the two instabilities to rapidly grow over comparable timescales. Interestingly, the same survey revealed that both mechanisms persist at long times, leading to a semi-stationary regime consistent with a spatially heterogeneous phase<sup>79,80</sup>: A quantum emulsion where paired and unpaired fermions macroscopically coexist while featuring phase segregation at the micro-scale of few interparticle spacings. It is interesting to remark how a similar spontaneous emergence of spatially-inhomogeneous states occurs in strongly-correlated electron systems: The simultaneous presence of multiple interaction mechanisms and the concurrence of distinct competing instabilities foster the emergence of nanometer-scale heterogeneous structures that host different phases and order parameters<sup>213,214</sup>.

While the study of repulsive Fermi mixtures has focused mainly on homonuclear systems, we remark that well-defined repulsive polarons – the building blocks of a repulsive Fermi liquid – were first revealed in mass-imbalanced  $^6\text{Li}-^{40}\text{K}$  FF mixtures<sup>163</sup>. It is also important to notice how a strong mass-asymmetry may greatly facilitate the development of macroscopic magnetic domains within a repulsive FF mixture: On the one hand, the reduced Fermi pressure of the heavy component can sizeably reduce the critical repulsion for ferromagnetism to emerge<sup>215</sup>. On the other hand, the pairing rate strongly depends upon the mass ratio of the two components, and it can be starkly decreased, respect to the equal-mass case<sup>82</sup>.

### Bose-Bose

As anticipated while describing Fig. 2, two condensates can either mix together occupying the whole available volume, separate in different domains, or collapse<sup>216</sup>. Since the study of the unitary Bose gas is limited to far-from-equilibrium dynamics<sup>217,218</sup>

due to the strong atom losses, we consider here a BB mixture of two independently stable gases (finite and positive  $a_1$  and  $a_2$ ) characterized by an intercomponent scattering length  $a_{12}$  (positive or negative) of the order of the intracomponent ones, and discuss the possible scenarios in the miscible and immiscible regimes, illustrated in Fig. 6 for the case of equal masses for the two components.

In the miscible regime ( $a_{12}^2 < |a_1 a_2|$ ), if the trapping potential is not flat, the two gases have equal ground state spatial profiles when  $a_1 = a_2$ <sup>219</sup>, whereas for  $a_1 \neq a_2$ , buoyancy effects come into play with the least repulsive gas concentrating towards the trap minimum and the other gas redistributing in the outer regions<sup>88</sup> (see examples in Fig. 6). The many-body mixture configuration and dynamics can be conveniently described introducing the total density ( $n = n_1 + n_2$ ) and their density difference, or magnetization ( $m = n_1 - n_2$ ). These two channels correspond to the in-phase and out-of-phase excitations of the mixture. Figure 6 shows examples of density distributions of both components for different  $a_1/a_2$  combinations and different  $\gamma$ , specifically around the critical values  $\gamma = \pm 1$ . Note that at  $\gamma = 0$  each component has a pure Thomas-Fermi profile, with radii associated to their own scattering length. Approaching  $\gamma = -1$ , the total density is strongly enhanced, consistently with a divergence in the compressibility  $\kappa$ . As  $\gamma$  tends to +1, instead, the total density is barely affected, while the magnetization shows a peak, in agreement with a divergence of the magnetic susceptibility  $\chi$ . The specific features of total density and magnetization channels, such as the interaction energy scales, the speeds of sound, and the healing lengths<sup>29</sup>, depend on the interaction constants and on the densities. In the particular case of equal masses, densities and intracomponent interactions ( $a_1 = a_2 = \bar{a}$ ), the ratio between the quantities associated to total density and magnetization channels is a function of  $(\bar{a} + a_{12})/(\bar{a} - a_{12})$ . The larger the difference between the two channels, the more they decouple and independent investigations can be implemented in a clean environment<sup>219–221</sup>. In general, though, complex many-body dynamics emerges causing damping and oscillation frequency<sup>71,222</sup> changes or turbulence<sup>223</sup>.

In the immiscible regime ( $a_{12} > \sqrt{a_1 a_2}$ ), bosonic mixture spatially self-organize in different single-component domains in order to minimize the energy cost associated to the strong intercomponent repulsion<sup>224</sup>. Beyond-mean-field effects can also lead to equilibrium configurations with bubbles of mixed phases coexisting with pure phase of one of the two components in case of either mass imbalance or different intracomponent interactions<sup>225</sup>. Note that immiscibility and magnetization excitations can only be observed in extended systems with a characteristic size that exceeds the magnetization healing length. Such features are instead inhibited in systems smaller than the healing length<sup>226,227</sup>.

Thanks to buoyancy and immiscibility, quantum mixtures support an extremely rich variety of topological defects such as different kinds of solitons<sup>228</sup> and vortices, compared to the case of single component gases. Exotic solitons<sup>229,230</sup>, soliton

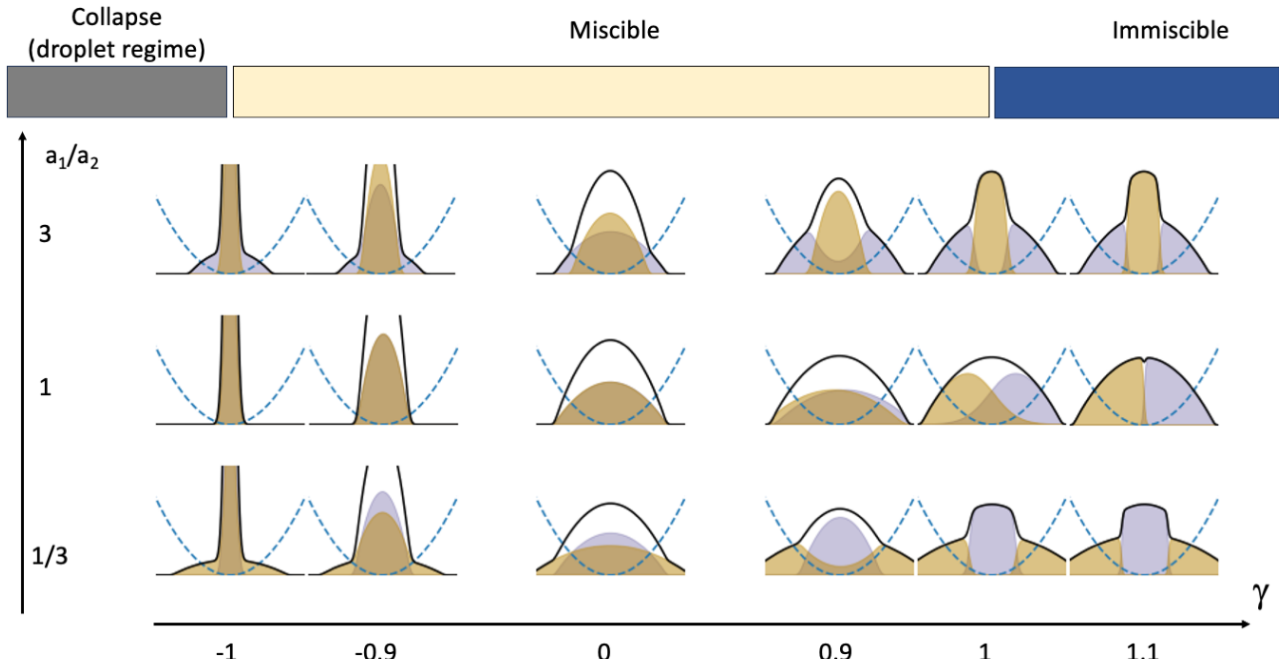


**Figure 6. Miscibility and buoyancy.** GPE simulation of the density distribution for a BB mixture, with equal masses of the constituents, in a harmonic trap (dashed) for different  $a_1/a_2$  and  $\gamma$  ( $a_2$  is kept fixed). Shaded colored regions illustrate the individual densities, while the solid line shows the total density. A small gradient was added to break the left-right symmetry.

trains<sup>231</sup>, magnetic solitons<sup>232,233</sup>, half quantum vortices<sup>234</sup> and stable massive multicharged vortices<sup>235</sup> are some of the topological structures that cannot be found in single component condensates.

In the special case of homonuclear spin mixtures, the presence of a coherent coupling radiation between two internal states, makes the individual phases lock one to each other and allows for state interconversion (spin is no longer conserved). The mixture state can be described with the Bloch vector formalism and treated in analogy with spin dipoles in the presence of an effective magnetic field following Landau-Lifshitz formalism<sup>236</sup> in the continuum. Such a coupled system is also suitable for investigating confinement physics in analogy to high-energy physics, since pairs of half quantum vortices behave in a very similar way to quark pairs<sup>45,237</sup>. If the difference between the mean intracomponent interactions and the intercomponent one is negative, the mixture shows a para- to ferromagnetic transition that can be studied and used for investigating magnetism in superfluid systems<sup>39,41</sup> as well as simulating quantum field theory predictions such as false vacuum decay<sup>238</sup> or cosmological curved space-time geometries<sup>239</sup>. When the states are coupled via a two-photon Raman transition with a non-negligible relative momentum, external and internal degrees of freedom couple (spin-orbit coupling) and the gas behave as in the presence of synthetic magnetic fields<sup>49,240</sup> and can exhibit supersolid features<sup>241</sup>.

When intracomponent interactions are attractive and stronger than the mean of the intracomponent ones ( $a_{12} < -\sqrt{a_1 a_2}$ ), mixtures can either form stable configurations or undergo collapse. Quantum droplets are self-bound many-body states that exist for small numbers of atoms up to a critical interaction strength, when  $a_{12}^2 \sim a_1 a_2$ . Originally predicted by D. Petrov<sup>93</sup> as a result of beyond mean-field effects, they were then observed in mixtures of different spin states of <sup>39</sup>K atoms<sup>90,91</sup> and in heteronuclear mixtures of KRb<sup>92</sup>. In one-dimensional geometry also bright soliton solutions, where dispersion compensates for attractive interactions, have been observed<sup>89</sup>.

Including the possibility to have a finite mass imbalance between the two components, new possible phases arise involving bubbles of mixed phases coexisting with a pure phase of one of the two components<sup>225</sup>.

### Fermi-Bose

As anticipated in the introduction, Fermi-Bose mixtures share many features with the BB ones. The first FB mixtures that have been brought to double quantum degeneracy are <sup>6</sup>Li-<sup>7</sup>Li<sup>58,59</sup>, <sup>40</sup>K-<sup>87</sup>Rb<sup>242-244</sup>, and <sup>6</sup>Li-<sup>23</sup>Na<sup>245</sup>. In Ref.<sup>37</sup> the reader can find a summary of most of the FB mixtures used nowadays and their peculiarities. We can identify two type of FB mixtures: In one case, the fermionic part can be given by a FF mixture itself, which can be brought in the superfluid regime, having de facto a BB mixture of two superfluids<sup>246</sup>. In the other case, the mixture is exquisitely Fermi-Bose, meaning that the fermionic part is given by a polarized degenerate Fermi gas. In this case, similarly to the BB case, the system can undergo phase separation<sup>247-249</sup> or collapse<sup>97</sup>, but also novel possibilities can arise, i.e., tailoring interactions between the fermionic component thanks to the mediation of the bosonic part<sup>250,251</sup>, or, viceversa, creating long range interactions between bosons mediated by the fermions<sup>252-254</sup>.

## Conclusions and Perspectives

In this review article, we provided an introductory overview of (some of) the physical phenomena and main experimental progress in the research field on ultracold quantum mixtures, from the three relevant perspectives of few-body physics, impurity problems, and many-body physics. The wealth of possible states arising in these three different sectors and the intertwining of few-to-many-body physics were discussed by taking into account both the role of a mass asymmetry and distinct quantum statistics of the mixture constituents, which lead to striking differences in the ultracold regime.

As anticipated in the Introduction, we intentionally restricted our discussion to bulk systems confined in three-dimensional potentials, only marginally mentioning the extremely rich fields of research on ultracold atomic mixtures in optical lattices<sup>2,3</sup>, reduced<sup>255,256</sup> or extended (synthetic)<sup>257,258</sup> dimensionality. Additionally, here we focused on the simplest, and most standard case of contact *s*-wave interactions between the two components: We emphasize that a wealth of phenomena and applications, not discussed in this work, are expected to emerge when higher-order (e.g. *p*- or *d*-wave) partial waves<sup>259</sup>, or long range interactions – such as dipolar ones<sup>260</sup> – are considered. In this context, it is also relevant to mention the important experimental progress in producing ultracold atom-ion mixtures<sup>34,35</sup>, and in manipulating their intercomponent interactions<sup>261</sup>.

Homonuclear spin mixtures (both bosonic and fermionic) have demonstrated to represent very powerful and highly-tunable platforms. They have allowed to achieve the first experimental implementation of a superfluid mixture and to widely investigate their rich many-body dynamics. In this context, interesting directions are offered by further exploration of spinor physics with nontrivial ground state configurations and excitations<sup>51</sup>, and the use of coherent coupling between internal states with and without spin-orbit coupling<sup>50</sup>, to generate highly-tunable quantum simulators with which to tackle a variety of phenomena belonging to other fields of physics, such as cosmology and gravitation<sup>262-265</sup>, magnetism<sup>221</sup>, and high energy physics<sup>237</sup>. Ultracold spin mixtures can also reveal their high potential for the implementation of spintronic devices with superfluid features, where the spin introduces an extra degree of freedom with respect to atomtronic applications<sup>266</sup>.

Heteronuclear mixtures offer the possibility to engineer species-selective optical potentials for an almost independent manipulation of the different components<sup>68</sup>. This allows not only to control the single species separately in terms of motion, density and momentum distributions, or tunneling rate, but also to explore mix-dimensional systems<sup>267–269</sup>, in which one component experiences a different dimensionality with respect to the other. Although progress has been already done in this context<sup>70,270</sup>, a wealth of predicted few- and many-body regimes still awaits experimental investigation.

As highlighted throughout our work, the presence of a mass asymmetry between the mixture constituents significantly enriches the physical scenarios that can be accessed, enabling the observation of novel states of quantum matter in the context of few-body systems, impurity physics, and many-body physics. In this regard, the recent progress in producing novel FF mixtures<sup>135,271</sup> and FF Feshbach dimers<sup>136,138</sup> is extremely appealing from several viewpoints. The intrinsic mismatch in the dispersion relations of the two components arising from the unequal masses could foster paradigmatic states of exotic superfluidity<sup>66,209,272</sup>. Moreover, stable few-body cluster states could be observed in both <sup>6</sup>Li-<sup>53</sup>Cr and <sup>40</sup>K-<sup>161</sup>Dy systems<sup>129,140,142,273</sup>. Besides representing an important step forward in the few-body context, these could represent a qualitative new opportunity to introduce non-perturbative elastic few-body correlations in fermionic media. In turn, these could promote novel types of impurity problems<sup>155,156</sup>, and trigger the emergence of exotic superfluid and normal states<sup>131,132</sup>.

Another rapidly developing field, strongly connected with the one of quantum mixtures, concerns ultracold ground-state polar molecules<sup>22,32,33</sup>, which can be realized through a two-step process, based on the association of heteronuclear atom pairs into Feshbach dimers, which are subsequently transferred to deeply-bound states via coherent optical schemes. Such molecular gases, with which both Fermi and Bose quantum degeneracy has been already achieved<sup>101,107,108</sup>, set the basis for countless applications and fundamental research: From novel quantum simulation and computation schemes based on the exploitation of long-ranged, tunable dipolar interactions, to controlled quantum chemistry and precision measurements.

To conclude, the field of ultracold quantum mixtures, established shortly after the advent of single-species quantum gases, has experienced an impressive progress over the last two decades, evolving over the years into a variety of diverse, cross-disciplinary research directions, only partially covered by this work. Far from being exhausted, this research area still offers a wealth of possibilities for future investigation and further developments, and we hope that this short overview will also help motivate young scientists to pursue their experimental and theoretical studies on ultracold quantum mixtures.

## Acknowledgements

We thank X. Cui, R. Grimm, D.S. Petrov, and P. Massignan for their critical reading of the manuscript, and the members of LENS Quantum Gases group in Florence and of the Pitaevskii BEC Center in Trento for fruitful discussions. We acknowledge financial support by the PE0000023-NQSTI project by the Italian Ministry of University and Research, co-funded by the European Union — NextGeneration EU. C.B and G.L. acknowledge financial support from Provincia Autonoma di Trento, and M.Z. acknowledges financial support from the ‘Integrated infrastructure initiative in Photonic and Quantum Sciences’ I-PHOQS (CUP B53C22001750006).

## Author contributions

All authors equally contributed to all aspects of the article.

## Competing interests

The authors declare no competing interests.

## Publisher’s note

Springer Nature remains neutral with regard to jurisdictional claims in published maps and institutional affiliations.

## References

1. Lewenstein, M. *et al.* Ultracold atomic gases in optical lattices: mimicking condensed matter physics and beyond. *Adv. Phys.* **56**, 243 – 379 (2007).
2. Gross, C. & Bloch, I. Quantum simulations with ultracold atoms in optical lattices. *Science* **357**, 995–1001, DOI: [10.1126/science.aal3837](https://doi.org/10.1126/science.aal3837) (2017). <https://www.science.org/doi/10.1126/science.aal3837>.
3. Schäfer, F., Fukuhara, T., Sugawa, S., Takasu, Y. & Takahashi, Y. Tools for quantum simulation with ultracold atoms in optical lattices. *Nat. Rev. Phys.* **2**, 411–425, DOI: [10.1038/s42254-020-0195-3](https://doi.org/10.1038/s42254-020-0195-3) (2020).
4. Sowiński, T. & García-March, M. A. One-dimensional mixtures of several ultracold atoms: a review. *Rep. Prog. Phys.* **82**, 104401, DOI: [DOI10.1088/1361-6633/ab3a80](https://doi.org/10.1088/1361-6633/ab3a80) (2019).
5. Mistakidis, S. *et al.* Few-body Bose gases in low dimensions—A laboratory for quantum dynamics. *Phys. Reports* **1042**, 1–108, DOI: <https://doi.org/10.1016/j.physrep.2023.10.004> (2023). Few-body Bose gases in low dimensions—A laboratory for quantum dynamics.
6. Bose, S. Plancks Gesetz und Lichtquantenhypothese. *Zeitschrift für Physik* **26**, 178–181, DOI: [10.1007/BF01327326](https://doi.org/10.1007/BF01327326) (1924).
7. Einstein, A. Quantentheorie des einatomigen idealen Gases I. *Sitzungsberichte der Preussischen Akademie der Wissenschaften* **21**, 261 (1924).
8. London, F. The  $\lambda$ -Phenomenon of Liquid Helium and the Bose-Einstein Degeneracy. *Nature* **141**, 643–644, DOI: [10.1038/141643a0](https://doi.org/10.1038/141643a0) (1938).
9. Fermi, E. Sulla quantizzazione del gas perfetto monoatomico. *Rendiconti Lincei* **3**, 145–149 (1926).
10. Dirac, P. A. M. On the theory of quantum mechanics. *Proc. R. Soc. Lond. A* **112**, 661–677, DOI: [http://doi.org/10.1098/rspa.1926.0133](https://doi.org/10.1098/rspa.1926.0133) (1926).
11. Pauli, W. Über den Zusammenhang des Abschlusses der Elektronengruppen im Atom mit der Komplexstruktur der Spektren. *Zeitschrift für Physik* **31**, 765–783 (1925).
12. Anderson, M. H., Ensher, J. R., Matthews, M. R., Wieman, C. E. & Cornell, E. A. Observation of Bose-Einstein condensation in dilute atomic vapor. *Science* **269**, 198–201, DOI: [10.1126/science.269.5221.198](https://doi.org/10.1126/science.269.5221.198) (1995).
13. Davis, K. B. *et al.* Bose-Einstein condensation in a gas of sodium atoms. *Phys. Rev. Lett.* **75**, 3969–3973, DOI: [10.1103/PhysRevLett.75.3969](https://doi.org/10.1103/PhysRevLett.75.3969) (1995).
14. DeMarco, B. & Jin, D. S. Onset of Fermi Degeneracy in a Trapped Atomic Gas. *Science* **285**, 1703–1706, DOI: [10.1126/science.285.5434.1703](https://doi.org/10.1126/science.285.5434.1703) (1999).
15. Ketterle, W., Durfee, D. S. & Stamper-Kurn, D. M. Making, probing and understanding Bose-Einstein condensates. *Proc. Int. Sch. Phys. - Enrico Fermi* **67** (1999). ArXiv:cond-mat/9904034.
16. Ketterle, W. & Zwierlein, M. W. Making, probing and understanding ultracold Fermi gases. *Rivista del Nuovo Cimento* **31**, 247–422 (2008).
17. Bloch, I., Dalibard, J. & Zwerger, W. Many-body physics with ultracold gases. *Rev. Mod. Phys.* **80**, 885, DOI: [10.1103/RevModPhys.80.885](https://doi.org/10.1103/RevModPhys.80.885) (2008).
18. Zwerger, W. (ed.) *The BCS-BEC Crossover and the Unitary Fermi Gas* (Springer, Berlin Heidelberg, 2012).
19. Chin, C., Grimm, R., Julienne, P. S. & Tiesinga, E. Feshbach resonances in ultracold gases. *Rev. Mod. Phys.* **82**, 1225–1286, DOI: [doi.org/10.1103/RevModPhys.82.1225](https://doi.org/10.1103/RevModPhys.82.1225) (2010).
20. Stan, C. A., Zwierlein, M. W., Schunck, C. H., Raupach, S. M. F. & Ketterle, W. Observation of Feshbach Resonances between Two Different Atomic Species. *Phys. Rev. Lett.* **93** (2004).
21. Inouye, S. *et al.* Observation of Heteronuclear Feshbach Resonances in a Mixture of Bosons and Fermions. *Phys. Rev. Lett.* **93**, 183201 (2004).
22. Carr, L. D., DeMille, D., Krems, R. V. & Ye, J. Cold and ultracold molecules: Science, technology and applications. *New J. Phys.* **11**, 055049, DOI: [10.1088/1367-2630/11/5/055049](https://doi.org/10.1088/1367-2630/11/5/055049) (2009).
23. Schirotzek, A., Wu, C.-H., Sommer, A. & Zwierlein, M. W. Observation of Fermi Polarons in a Tunable Fermi Liquid of Ultracold Atoms. *Phys. Rev. Lett.* **102**, 230402, DOI: [10.1103/PhysRevLett.102.230402](https://doi.org/10.1103/PhysRevLett.102.230402) (2009).
24. Spethmann, N. *et al.* Dynamics of Single Neutral Impurity Atoms Immersed in an Ultracold Gas. *Phys. Rev. Lett.* **109**, 235301, DOI: [10.1103/PhysRevLett.109.235301](https://doi.org/10.1103/PhysRevLett.109.235301) (2012).

25. Timmermans, E. Phase Separation of Bose-Einstein Condensates. *Phys. Rev. Lett.* **81**, 5718–5721, DOI: [10.1103/PhysRevLett.81.5718](https://doi.org/10.1103/PhysRevLett.81.5718) (1998).
26. Ao, P. & Chu, S. T. Binary Bose-Einstein condensate mixtures in weakly and strongly segregated phases. *Phys. Rev. A* **58**, 4836–4840, DOI: [10.1103/PhysRevA.58.4836](https://doi.org/10.1103/PhysRevA.58.4836) (1998).
27. Trippenbach, M., Góral, K., Rzazewski, K., Malomed, B. & Band, Y. B. Structure of binary Bose-Einstein condensates. *J. Phys. B: At. Mol. Opt. Phys.* **33**, 4017, DOI: [10.1088/0953-4075/33/19/314](https://doi.org/10.1088/0953-4075/33/19/314) (2000).
28. Grimm, R. & Baroni, C. *Fermionic quantum mixtures with tunable interactions* (Proceedings of the International School of Physics "Enrico Fermi", Course 211 "Quantum Mixtures with Ultra-cold Atoms", IOS Press, Amsterdam; SIF, Bologna, 2024). [arXiv:2311.01220](https://arxiv.org/abs/2311.01220).
29. Lamporesi, G. *Two-component spin mixtures* (Proceedings of the International School of Physics "Enrico Fermi", Course 211 "Quantum Mixtures with Ultra-cold Atoms", IOS Press, Amsterdam; SIF, Bologna, 2024). [arXiv:2304.03711](https://arxiv.org/abs/2304.03711).
30. Zaccanti, M. *Mass-imbalanced Fermi mixtures with resonant interactions* (Proceedings of the International School of Physics "Enrico Fermi", Course 211 "Quantum Mixtures with Ultra-cold Atoms", IOS Press, Amsterdam; SIF, Bologna, 2024). [arXiv:2306.02736](https://arxiv.org/abs/2306.02736).
31. Schäfer, F., Fukuhara, T., Sugawa, S., Takasu, Y. & Takahashi, Y. Tools for quantum simulation with ultracold atoms in optical lattices. *Nat. Rev. Phys.* **2**, 411–425, DOI: [10.1038/s42254-020-0195-3](https://doi.org/10.1038/s42254-020-0195-3) (2020).
32. Quéméner, G. & Julienne, P. S. Ultracold molecules under control! *Chem. Rev.* **112**, 4949–5011, DOI: [10.1021/cr300092g](https://doi.org/10.1021/cr300092g) (2012). PMID: 22921011, <https://doi.org/10.1021/cr300092g>.
33. Langen, T., Valtolina, G., Wang, D. & Ye, J. Quantum state manipulation and science of ultracold molecules (2023). [2305.13445](https://arxiv.org/abs/2305.13445).
34. Tomza, M. *et al.* Cold hybrid ion-atom systems. *Rev. Mod. Phys.* **91**, 035001, DOI: [10.1103/RevModPhys.91.035001](https://doi.org/10.1103/RevModPhys.91.035001) (2019).
35. Lous, R. S. & Gerritsma, R. Chapter two - ultracold ion-atom experiments: cooling, chemistry, and quantum effects. In DiMauro, L. F., Perrin, H. & Yelin, S. F. (eds.) *Advances in Atomic, Molecular, and Optical Physics*, vol. 71 of *Advances In Atomic, Molecular, and Optical Physics*, 65–133, DOI: <https://doi.org/10.1016/bs.aamop.2022.05.002> (Academic Press, 2022).
36. Myatt, C. J., Burt, E. A., Ghrist, R. W., Cornell, E. A. & Wieman, C. E. Production of Two Overlapping Bose-Einstein Condensates by Sympathetic Cooling. *Phys. Rev. Lett.* **78**, 586–589, DOI: [10.1103/PhysRevLett.78.586](https://doi.org/10.1103/PhysRevLett.78.586) (1997).
37. Onofrio, R. Physics of our Days: Cooling and thermometry of atomic Fermi gases. *Physics-Uspekhi* **59**, 1129, DOI: [10.3367/UFNe.2016.07.037873](https://doi.org/10.3367/UFNe.2016.07.037873) (2016).
38. Gerbier, F., Widera, A., Fölling, S., Mandel, O. & Bloch, I. Resonant control of spin dynamics in ultracold quantum gases by microwave dressing. *Phys. Rev. A* **73**, 041602, DOI: [10.1103/PhysRevA.73.041602](https://doi.org/10.1103/PhysRevA.73.041602) (2006).
39. Zibold, T., Nicklas, E., Gross, C. & Oberthaler, M. K. Classical Bifurcation at the Transition from Rabi to Josephson Dynamics. *Phys. Rev. Lett.* **105**, 204101, DOI: [10.1103/PhysRevLett.105.204101](https://doi.org/10.1103/PhysRevLett.105.204101) (2010).
40. Nicklas, E. *et al.* Observation of scaling in the dynamics of a strongly quenched quantum gas. *Phys. Rev. Lett.* **115**, 245301, DOI: [10.1103/PhysRevLett.115.245301](https://doi.org/10.1103/PhysRevLett.115.245301) (2015).
41. Cominotti, R. *et al.* Ferromagnetism in an Extended Coherently Coupled Atomic Superfluid. *Phys. Rev. X* **13**, 021037, DOI: [10.1103/PhysRevX.13.021037](https://doi.org/10.1103/PhysRevX.13.021037) (2023).
42. Mancini, M. *et al.* Observation of chiral edge states with neutral fermions in synthetic hall ribbons. *Science* **349**, 1510–1513, DOI: [10.1126/science.aaa8736](https://doi.org/10.1126/science.aaa8736) (2015).
43. Stuhl, B. K., Lu, H.-I., Aycock, L. M., Genkina, D. & Spielman, I. B. Visualizing edge states with an atomic bose gas in the quantum hall regime. *Science* **349**, 1514–1518, DOI: [10.1126/science.aaa8515](https://doi.org/10.1126/science.aaa8515) (2015). <https://www.science.org/doi/pdf/10.1126/science.aaa8515>.
44. Bouhiron, J.-B. *et al.* Realization of an atomic quantum hall system in four dimensions. *Science* **384**, 223–227, DOI: [10.1126/science.adf8459](https://doi.org/10.1126/science.adf8459) (2024). <https://www.science.org/doi/pdf/10.1126/science.adf8459>.
45. Son, D. T. & Stephanov, M. A. Domain walls of relative phase in two-component Bose-Einstein condensates. *Phys. Rev. A* **65**, 063621, DOI: [10.1103/PhysRevA.65.063621](https://doi.org/10.1103/PhysRevA.65.063621) (2002).

46. Gallemí, A., Pitaevskii, L. P., Stringari, S. & Recati, A. Decay of the relative phase domain wall into confined vortex pairs: The case of a coherently coupled bosonic mixture. *Phys. Rev. A* **100**, 023607, DOI: [10.1103/PhysRevA.100.023607](https://doi.org/10.1103/PhysRevA.100.023607) (2019).

47. Frölian, A. *et al.* Realizing a 1d topological gauge theory in an optically dressed bec. *Nature* **608**, 293–297, DOI: [10.1038/s41586-022-04943-3](https://doi.org/10.1038/s41586-022-04943-3) (2022).

48. Weinfurtner, S., Liberati, S. & Visser, M. *Analogue Space-time Based on 2-Component Bose-Einstein Condensates* (Springer Berlin Heidelberg, Berlin, Heidelberg, 2007).

49. Lin, Y.-J., Jimenez-Garcia, K. & Spielman, I. B. Spin-orbit-coupled Bose-Einstein condensates. *Nat. (London)* **471**, 83–86, DOI: [10.1038/nature09887](https://doi.org/10.1038/nature09887) (2011).

50. Recati, A. & Stringari, S. Coherently coupled mixtures of ultracold atomic gases. *Annu. Rev. Condens. Matter Phys.* **13**, 407–432, DOI: [10.1146/annurev-conmatphys-031820-121316](https://doi.org/10.1146/annurev-conmatphys-031820-121316) (2022).

51. Stamper-Kurn, D. M. & Ueda, M. Spinor bose gases: Symmetries, magnetism, and quantum dynamics. *Rev. Mod. Phys.* **85**, 1191–1244, DOI: [10.1103/RevModPhys.85.1191](https://doi.org/10.1103/RevModPhys.85.1191) (2013).

52. Stenger, J. *et al.* Spin domains in ground-state Bose–Einstein condensates. *Nature* **396**, 345–348, DOI: [10.1038/24567](https://doi.org/10.1038/24567) (1998).

53. Jiménez-García, K. *et al.* Spontaneous formation and relaxation of spin domains in antiferromagnetic spin-1 condensates. *Nat. Commun.* **10**, 1422, DOI: [10.1038/s41467-019-10850-6](https://doi.org/10.1038/s41467-019-10850-6) (2019).

54. Barrett, M. D., Sauer, J. A. & Chapman, M. S. All-Optical Formation of an Atomic Bose-Einstein Condensate. *Phys. Rev. Lett.* **87**, 010404 (2001).

55. Chang, M.-S. *et al.* Observation of Spinor Dynamics in Optically Trapped  $^{87}\text{Rb}$  Bose-Einstein Condensates. *Phys. Rev. Lett.* **92**, 140403, DOI: [10.1103/PhysRevLett.92.140403](https://doi.org/10.1103/PhysRevLett.92.140403) (2004).

56. Pagano, G. *et al.* A one-dimensional liquid of fermions with tunable spin. *Nat. Phys.* **10**, 198–201, DOI: [10.1038/nphys2878](https://doi.org/10.1038/nphys2878) (2014).

57. Modugno, G. *et al.* Bose-Einstein Condensation of Potassium Atoms by Sympathetic Cooling. *Science* **294**, 1320–1322, DOI: [10.1126/science.1066687](https://doi.org/10.1126/science.1066687) (2001).

58. Schreck, F. *et al.* Quasipure Bose-Einstein Condensate Immersed in a Fermi Sea. *Phys. Rev. Lett.* **87**, 080403, DOI: [10.1103/PhysRevLett.87.080403](https://doi.org/10.1103/PhysRevLett.87.080403) (2001).

59. Truscott, A. G., Strecker, K. E., McAlexander, W. I., Partridge, G. B. & Hulet, R. G. Observation of Fermi Pressure in a Gas of Trapped Atoms. *Science* **291**, 2570–2572, DOI: [10.1126/science.1059318](https://doi.org/10.1126/science.1059318) (2001).

60. Taglieber, M., Voigt, A.-C., Aoki, T., Hänsch, T. W. & Dieckmann, K. Quantum Degenerate Two-Species Fermi-Fermi Mixture Coexisting with a Bose-Einstein Condensate. *Phys. Rev. Lett.* **100**, 010401, DOI: [10.1103/PhysRevLett.100.010401](https://doi.org/10.1103/PhysRevLett.100.010401) (2008).

61. Wille, E. *et al.* Exploring an Ultracold Fermi-Fermi Mixture: Interspecies Feshbach Resonances and Scattering Properties of  $^6\text{Li}$  and  $^{40}\text{K}$ . *Phys. Rev. Lett.* **100**, 053201, DOI: [10.1103/PhysRevLett.100.053201](https://doi.org/10.1103/PhysRevLett.100.053201) (2008).

62. Tung, S.-K. *et al.* Ultracold mixtures of atomic  $^6\text{Li}$  and  $^{133}\text{Cs}$  with tunable interactions. *Phys. Rev. A* **87**, 010702, DOI: [10.1103/PhysRevA.87.010702](https://doi.org/10.1103/PhysRevA.87.010702) (2013).

63. Green, A. *et al.* Feshbach Resonances in  $p$ -Wave Three-Body Recombination within Fermi-Fermi Mixtures of Open-Shell  $^6\text{Li}$  and Closed-Shell  $^{173}\text{Yb}$  Atoms. *Phys. Rev. X* **10**, 031037, DOI: [10.1103/PhysRevX.10.031037](https://doi.org/10.1103/PhysRevX.10.031037) (2020).

64. Naidon, P. & Endo, S. Efimov physics: a review. *Rep. Prog. Phys.* **80**, 056001, DOI: [10.1088/1361-6633/aa50e8](https://doi.org/10.1088/1361-6633/aa50e8) (2017).

65. Chevy, F. & Mora, C. Ultra-cold polarized Fermi gases. *Rep. Prog. Phys.* **73**, 112401 (2010).

66. Baarsma, J. E., Gubbels, K. B. & Stoof, H. T. C. Population and mass imbalance in atomic Fermi gases. *Phys. Rev. A* **82**, 013624, DOI: [10.1103/PhysRevA.82.013624](https://doi.org/10.1103/PhysRevA.82.013624) (2010).

67. Grimm, R., Weidemüller, M. & Ovchinnikov, Y. B. Optical dipole traps for neutral atoms. *Adv. At. Mol. Opt. Phys.* **42**, 95, DOI: [10.1016/S1049-250X\(08\)60186-X](https://doi.org/10.1016/S1049-250X(08)60186-X) (2000).

68. LeBlanc, L. J. & Thywissen, J. H. Species-specific optical lattices. *Phys. Rev. A* **75**, 053612, DOI: [10.1103/PhysRevA.75.053612](https://doi.org/10.1103/PhysRevA.75.053612) (2007).

69. Catani, J. *et al.* Entropy Exchange in a Mixture of Ultracold Atoms. *Phys. Rev. Lett.* **103**, 140401, DOI: [10.1103/PhysRevLett.103.140401](https://doi.org/10.1103/PhysRevLett.103.140401) (2009).

70. Lamporesi, G. *et al.* Scattering in mixed dimensions with ultracold gases. *Phys. Rev. Lett.* **104**, 153202, DOI: [10.1103/PhysRevLett.104.153202](https://doi.org/10.1103/PhysRevLett.104.153202) (2010).
71. Wilson, K. E., Guttridge, A., Segal, J. & Cornish, S. L. Quantum degenerate mixtures of Cs and Yb. *Phys. Rev. A* **103**, 033306, DOI: [10.1103/PhysRevA.103.033306](https://doi.org/10.1103/PhysRevA.103.033306) (2021).
72. Elliott, E. R. *et al.* Quantum gas mixtures and dual-species atom interferometry in space. *Nature* **623**, 502–508, DOI: [10.1038/s41586-023-06645-w](https://doi.org/10.1038/s41586-023-06645-w) (2023).
73. Stoner, E. Atomic moments in ferromagnetic metals and alloys with non-ferromagnetic elements. *Philos. Mag.* **15**, 1018–1034 (1933).
74. Duine, R. A. & MacDonald, A. H. Itinerant Ferromagnetism in an Ultracold Atom Fermi Gas. *Phys. Rev. Lett.* **95**, 230403, DOI: [10.1103/PhysRevLett.95.230403](https://doi.org/10.1103/PhysRevLett.95.230403) (2005).
75. Pilati, S., Bertaina, G., Giorgini, S. & Troyer, M. Itinerant Ferromagnetism of a Repulsive Atomic Fermi Gas: A Quantum Monte Carlo Study. *Phys. Rev. Lett.* **105**, 030405, DOI: [10.1103/PhysRevLett.105.030405](https://doi.org/10.1103/PhysRevLett.105.030405) (2010).
76. Chang, S.-Y., Randeria, M. & Trivedi, N. Ferromagnetism in the upper branch of the Feshbach resonance and the hard-sphere Fermi gas. *Proc. Nat. Acad. Sci.* **108**, 51–54, DOI: [10.1073/pnas.1011990108](https://doi.org/10.1073/pnas.1011990108) (2011).
77. Jo, G.-B. *et al.* Itinerant Ferromagnetism in a Fermi Gas of Ultracold Atoms. *Science* **325**, 1521–1524, DOI: [10.1126/science.1177112](https://doi.org/10.1126/science.1177112) (2009).
78. Valtolina, G. *et al.* Exploring the ferromagnetic behaviour of a repulsive Fermi gas through spin dynamics. *Nat. Phys.* **13**, 704–709, DOI: [10.1038/nphys4108](https://doi.org/10.1038/nphys4108) (2017).
79. Amico, A. *et al.* Time-Resolved Observation of Competing Attractive and Repulsive Short-Range Correlations in Strongly Interacting Fermi Gases. *Phys. Rev. Lett.* **121**, 253602, DOI: [10.1103/PhysRevLett.121.253602](https://doi.org/10.1103/PhysRevLett.121.253602) (2018).
80. Scazza, F. *et al.* Exploring emergent heterogeneous phases in strongly repulsive Fermi gases. *Phys. Rev. A* **101**, 013603, DOI: [10.1103/PhysRevA.101.013603](https://doi.org/10.1103/PhysRevA.101.013603) (2020).
81. Massignan, P., Zaccanti, M. & Bruun, G. M. Polarons, dressed molecules and itinerant ferromagnetism in ultracold Fermi gases. *Rep. Prog. Phys.* **77**, 034401, DOI: [10.1088/0034-4885/77/3/034401](https://doi.org/10.1088/0034-4885/77/3/034401) (2014).
82. Petrov, D. S. Three-body problem in Fermi gases with short-range interparticle interaction. *Phys. Rev. A* **67**, 010703, DOI: [10.1103/PhysRevA.67.010703](https://doi.org/10.1103/PhysRevA.67.010703) (2003).
83. Pekker, D. *et al.* Competition between Pairing and Ferromagnetic Instabilities in Ultracold Fermi Gases near Feshbach Resonances. *Phys. Rev. Lett.* **106**, 050402, DOI: [10.1103/PhysRevLett.106.050402](https://doi.org/10.1103/PhysRevLett.106.050402) (2011).
84. Shenoy, V. B. & Ho, T.-L. Nature and Properties of a Repulsive Fermi Gas in the Upper Branch of the Energy Spectrum. *Phys. Rev. Lett.* **107**, 210401, DOI: [10.1103/PhysRevLett.107.210401](https://doi.org/10.1103/PhysRevLett.107.210401) (2011).
85. Sanner, C. *et al.* Correlations and Pair Formation in a Repulsively Interacting Fermi Gas. *Phys. Rev. Lett.* **108**, 240404, DOI: [10.1103/PhysRevLett.108.240404](https://doi.org/10.1103/PhysRevLett.108.240404) (2012).
86. Scazza, F. *et al.* Repulsive Fermi Polarons in a Resonant Mixture of Ultracold  $^6\text{Li}$  Atoms. *Phys. Rev. Lett.* **118**, 083602, DOI: [10.1103/PhysRevLett.118.083602](https://doi.org/10.1103/PhysRevLett.118.083602) (2017).
87. Papp, S. B., Pino, J. M. & Wieman, C. E. Tunable Miscibility in a Dual-Species Bose-Einstein Condensate. *Phys. Rev. Lett.* **101**, 040402, DOI: [10.1103/PhysRevLett.101.040402](https://doi.org/10.1103/PhysRevLett.101.040402) (2008).
88. Hall, D. S., Matthews, M. R., Ensher, J. R., Wieman, C. E. & Cornell, E. A. Dynamics of Component Separation in a Binary Mixture of Bose-Einstein Condensates. *Phys. Rev. Lett.* **81**, 1539–1542, DOI: [10.1103/PhysRevLett.81.1539](https://doi.org/10.1103/PhysRevLett.81.1539) (1998).
89. Cheiney, P. *et al.* Bright Soliton to Quantum Droplet Transition in a Mixture of Bose-Einstein Condensates. *Phys. Rev. Lett.* **120**, 135301, DOI: [10.1103/PhysRevLett.120.135301](https://doi.org/10.1103/PhysRevLett.120.135301) (2018).
90. Cabrera, C. R. *et al.* Quantum liquid droplets in a mixture of Bose-Einstein condensates. *Science* **359**, 301–304, DOI: [10.1126/science.aaq5686](https://doi.org/10.1126/science.aaq5686) (2018). <https://www.science.org/doi/pdf/10.1126/science.aaq5686>.
91. Semeghini, G. *et al.* Self-bound quantum droplets of atomic mixtures in free space. *Phys. Rev. Lett.* **120**, 235301, DOI: [10.1103/PhysRevLett.120.235301](https://doi.org/10.1103/PhysRevLett.120.235301) (2018).
92. D'Errico, C. *et al.* Observation of quantum droplets in a heteronuclear bosonic mixture. *Phys. Rev. Res.* **1**, 033155, DOI: [10.1103/PhysRevResearch.1.033155](https://doi.org/10.1103/PhysRevResearch.1.033155) (2019).

93. Petrov, D. S. Quantum Mechanical Stabilization of a Collapsing Bose-Bose Mixture. *Phys. Rev. Lett.* **115**, 155302, DOI: [10.1103/PhysRevLett.115.155302](https://doi.org/10.1103/PhysRevLett.115.155302) (2015).

94. Wilson, K. E. *et al.* Dynamics of a degenerate cs-yb mixture with attractive interspecies interactions. *Phys. Rev. Res.* **3**, 033096, DOI: [10.1103/PhysRevResearch.3.033096](https://doi.org/10.1103/PhysRevResearch.3.033096) (2021).

95. Papp, S. B. & Wieman, C. E. Observation of Heteronuclear Feshbach Molecules from a  $^{85}\text{Rb}$ – $^{87}\text{Rb}$  Gas. *Phys. Rev. Lett.* **97**, 180404, DOI: [10.1103/PhysRevLett.97.180404](https://doi.org/10.1103/PhysRevLett.97.180404) (2006).

96. Lam, A. Z. *et al.* High phase-space density gas of NaCs Feshbach molecules. *Phys. Rev. Res.* **4**, L022019, DOI: [10.1103/PhysRevResearch.4.L022019](https://doi.org/10.1103/PhysRevResearch.4.L022019) (2022).

97. Modugno, G. *et al.* Collapse of a degenerate fermi gas. *Science* **297**, 2240–2243, DOI: [10.1126/science.1077386](https://doi.org/10.1126/science.1077386) (2002).

98. Ospelkaus, C., Ospelkaus, S., Sengstock, K. & Bongs, K. Interaction-driven dynamics of  $^{40}\text{K}$ – $^{87}\text{rb}$  fermion-boson gas mixtures in the large-particle-number limit. *Phys. Rev. Lett.* **96**, 020401, DOI: [10.1103/PhysRevLett.96.020401](https://doi.org/10.1103/PhysRevLett.96.020401) (2006).

99. Ospelkaus, S., Ospelkaus, C., Humbert, L., Sengstock, K. & Bongs, K. Tuning of heteronuclear interactions in a degenerate fermi-bose mixture. *Phys. Rev. Lett.* **97**, 120403, DOI: [10.1103/PhysRevLett.97.120403](https://doi.org/10.1103/PhysRevLett.97.120403) (2006).

100. Zaccanti, M. *et al.* Control of the interaction in a Fermi-Bose mixture. *Phys. Rev. A* **74**, 041605, DOI: [10.1103/PhysRevA.74.041605](https://doi.org/10.1103/PhysRevA.74.041605) (2006).

101. Duda, M. *et al.* Transition from a polaronic condensate to a degenerate Fermi gas of heteronuclear molecules. *Nat. Phys.* **19**, 720–725, DOI: [10.1038/s41567-023-01948-1](https://doi.org/10.1038/s41567-023-01948-1) (2023).

102. Ufrecht, C., Meister, M., Roura, A. & Schleich, W. P. Comprehensive classification for Bose–Fermi mixtures. *New J. Phys.* **19**, 085001, DOI: [10.1088/1367-2630/aa7814](https://doi.org/10.1088/1367-2630/aa7814) (2017).

103. Busch, T., Anglin, J. R., Cirac, J. I. & Zoller, P. Inhibition of spontaneous emission in Fermi gases. *Eur. Lett.* **44**, 1 (1998).

104. Pricoupenko, L. & Castin, Y. One particle in a box: The simplest model for a Fermi gas in the unitary limit. *Phys. Rev. A* **69**, 051601, DOI: [10.1103/PhysRevA.69.051601](https://doi.org/10.1103/PhysRevA.69.051601) (2004).

105. Köhler, T., Goral, K. & Julienne, P. S. Production of cold molecules via magnetically tunable Feshbach resonances. *Rev. Mod. Phys.* **78**, 1311, DOI: [10.1103/RevModPhys.78.1311](https://doi.org/10.1103/RevModPhys.78.1311) (2006).

106. Vitanov, N. V., Rangelov, A. A., Shore, B. W. & Bergmann, K. Stimulated Raman adiabatic passage in physics, chemistry, and beyond. *Rev. Mod. Phys.* **89**, 015006, DOI: [10.1103/RevModPhys.89.015006](https://doi.org/10.1103/RevModPhys.89.015006) (2017).

107. Valtolina, G. *et al.* Dipolar evaporation of reactive molecules to below the Fermi temperature. *Nature* **588**, 239–243, DOI: [10.1038/s41586-020-2980-7](https://doi.org/10.1038/s41586-020-2980-7) (2020).

108. Bigagli, N. *et al.* Observation of Bose-Einstein condensation of dipolar molecules. *arXiv:2312.10965* (2023).

109. Fonseca, A. C., Redish, E. F. & Shanley, P. Efimov effect in an analytically solvable model. *Nucl. Phys. A* **320**, 273–288, DOI: [https://doi.org/10.1016/0375-9474\(79\)90189-1](https://doi.org/10.1016/0375-9474(79)90189-1) (1979).

110. Efimov, V. Energy levels arising from resonant two-body forces in a three-body system. *Phys. Lett. B* **33**, 563–564 (1970).

111. Braaten, E. & Hammer, H.-W. Universality in few-body systems with large scattering length. *Phys. Rep.* **428**, 259–390 (2006).

112. Braaten, E. & Hammer, H. Efimov physics in cold atoms. *Ann. Phys.* **322**, 120–163 (2007).

113. Blume, D. Few-body physics with ultracold atomic and molecular systems in traps. *Reports on Prog. Phys.* **75**, 046401, DOI: [10.1088/0034-4885/75/4/046401](https://doi.org/10.1088/0034-4885/75/4/046401) (2012).

114. Wang, Y., D’Incao, J. P. & Esry, B. D. Chapter 1 - ultracold few-body systems. In Arimondo, E., Berman, P. R. & Lin, C. C. (eds.) *Advances in Atomic, Molecular, and Optical Physics*, vol. 62 of *Advances In Atomic, Molecular, and Optical Physics*, 1–115, DOI: <https://doi.org/10.1016/B978-0-12-408090-4.00001-3> (Academic Press, 2013).

115. Landau, L. D. & Lifshitz, E. M. *Quantum Mechanics, vol. 3 (Course of theoretical physics)* (Butterworth-Heinemann, Oxford, 1977).

116. Rem, B. S. *et al.* Lifetime of the Bose Gas with Resonant Interactions. *Phys. Rev. Lett.* **110**, 163202, DOI: [10.1103/PhysRevLett.110.163202](https://doi.org/10.1103/PhysRevLett.110.163202) (2013).

117. Fletcher, R. J., Gaunt, A. L., Navon, N., Smith, R. P. & Hadzibabic, Z. Stability of a Unitary Bose Gas. *Phys. Rev. Lett.* **111**, 125303, DOI: [10.1103/PhysRevLett.111.125303](https://doi.org/10.1103/PhysRevLett.111.125303) (2013).

118. Kraemer, T. *et al.* Evidence for Efimov quantum states in an ultracold gas of caesium atoms. *Nat. (London)* **440**, 315–318, DOI: [10.1038/nature04626](https://doi.org/10.1038/nature04626) (2006).

119. Ottenstein, T. B., Lompe, T., Kohnen, M., Wenz, A. N. & Jochim, S. Collisional stability of a three-component degenerate Fermi gas. *Phys. Rev. Lett.* **101**, 203202, DOI: [10.1103/PhysRevLett.101.203202](https://doi.org/10.1103/PhysRevLett.101.203202) (2008).

120. Lompe, T. *et al.* Atom-Dimer Scattering in a Three-Component Fermi Gas. *Phys. Rev. Lett.* **105**, 103201 (2010).

121. Lompe, T. *et al.* Radio-Frequency Association of Efimov Trimers. *Science* **330**, 940–944 (2010).

122. Huckans, J. H., Williams, J. R., Hazlett, E. L., Stites, R. W. & O’Hara, K. M. Three-body recombination in a three-state Fermi gas with widely tunable interactions. *Phys. Rev. Lett.* **102**, 165302, DOI: [10.1103/PhysRevLett.102.165302](https://doi.org/10.1103/PhysRevLett.102.165302) (2009).

123. Williams, J. R. *et al.* Evidence for an excited-state Efimov trimer in a three-component Fermi gas. *Phys. Rev. Lett.* **103**, 130404 (2009).

124. Barontini, G. *et al.* Observation of heteronuclear atomic Efimov resonances. *Phys. Rev. Lett.* **103**, 043201, DOI: [10.1103/PhysRevLett.103.043201](https://doi.org/10.1103/PhysRevLett.103.043201) (2009).

125. Bloom, R. S., Hu, M.-G., Cumby, T. D. & Jin, D. S. Tests of Universal Three-Body Physics in an Ultracold Bose-Fermi Mixture. *Phys. Rev. Lett.* **111**, 105301, DOI: [10.1103/PhysRevLett.111.105301](https://doi.org/10.1103/PhysRevLett.111.105301) (2013).

126. Pires, R. *et al.* Observation of Efimov Resonances in a Mixture with Extreme Mass Imbalance. *Phys. Rev. Lett.* **112**, 250404, DOI: [10.1103/PhysRevLett.112.250404](https://doi.org/10.1103/PhysRevLett.112.250404) (2014).

127. Tung, S.-K., Jiménez-García, K., Johansen, J., Parker, C. V. & Chin, C. Geometric Scaling of Efimov States in a  ${}^6\text{Li}$ – ${}^{133}\text{Cs}$  Mixture. *Phys. Rev. Lett.* **113**, 240402, DOI: [10.1103/PhysRevLett.113.240402](https://doi.org/10.1103/PhysRevLett.113.240402) (2014).

128. Maier, R. A. W., Eisele, M., Tiemann, E. & Zimmermann, C. Efimov Resonance and Three-Body Parameter in a Lithium-Rubidium Mixture. *Phys. Rev. Lett.* **115**, 043201, DOI: [10.1103/PhysRevLett.115.043201](https://doi.org/10.1103/PhysRevLett.115.043201) (2015).

129. Kartavtsev, O. I. & Malykh, A. V. Low-energy three-body dynamics in binary quantum gases. *J. Phys. B* **40**, 1429 (2007).

130. Endo, S., Naidon, P. & Ueda, M. Crossover trimers connecting continuous and discrete scaling regimes. *Phys. Rev. A* **86**, 062703, DOI: [10.1103/PhysRevA.86.062703](https://doi.org/10.1103/PhysRevA.86.062703) (2012).

131. Endo, S., García-García, A. M. & Naidon, P. Universal clusters as building blocks of stable quantum matter. *Phys. Rev. A* **93**, 053611, DOI: [10.1103/PhysRevA.93.053611](https://doi.org/10.1103/PhysRevA.93.053611) (2016).

132. Liu, R., Wang, W. & Cui, X. Quartet Superfluid in Two-Dimensional Mass-Imbalanced Fermi Mixtures. *Phys. Rev. Lett.* **131**, 193401, DOI: [10.1103/PhysRevLett.131.193401](https://doi.org/10.1103/PhysRevLett.131.193401) (2023).

133. Jag, M. *et al.* Observation of a Strong Atom-Dimer Attraction in a Mass-Imbalanced Fermi-Fermi Mixture. *Phys. Rev. Lett.* **112**, 075302, DOI: [10.1103/PhysRevLett.112.075302](https://doi.org/10.1103/PhysRevLett.112.075302) (2014).

134. Ciamei, A. *et al.* Double-degenerate fermi mixtures of  ${}^6\text{Li}$  and  ${}^{53}\text{Cr}$  atoms. *Phys. Rev. A* **106**, 053318, DOI: [10.1103/PhysRevA.106.053318](https://doi.org/10.1103/PhysRevA.106.053318) (2022).

135. Ciamei, A. *et al.* Exploring ultracold collisions in  ${}^6\text{Li}$ – ${}^{53}\text{Cr}$  fermi mixtures: Feshbach resonances and scattering properties of a novel alkali-transition metal system. *Phys. Rev. Lett.* **129**, 093402, DOI: [10.1103/PhysRevLett.129.093402](https://doi.org/10.1103/PhysRevLett.129.093402) (2022).

136. Finelli, S. *et al.* Ultracold LiCr: a new pathway to quantum gases of paramagnetic polar molecules (2024). [2402.08337](https://doi.org/10.4236/240208337).

137. Ravensbergen, C. *et al.* Resonantly Interacting Fermi-Fermi Mixture of  ${}^{161}\text{Dy}$  and  ${}^{40}\text{K}$ . *Phys. Rev. Lett.* **124**, 203402, DOI: [10.1103/PhysRevLett.124.203402](https://doi.org/10.1103/PhysRevLett.124.203402) (2020).

138. Soave, E. *et al.* Optically trapped feshbach molecules of fermionic  ${}^{161}\text{Dy}$  and  ${}^{40}\text{K}$ . *Phys. Rev. Res.* **5**, 033117, DOI: [10.1103/PhysRevResearch.5.033117](https://doi.org/10.1103/PhysRevResearch.5.033117) (2023).

139. Kartavtsev, O. I., Malykh, A. V. & Sofianos, S. A. Bound states and scattering lengths of three two-component particles with zero-range interactions under one-dimensional confinement. *J. Exp. Theor. Phys.* **108**, 365–373, DOI: [10.1134/S1063776109030017](https://doi.org/10.1134/S1063776109030017) (2009).

140. Pricoupenko, L. & Pedri, P. Universal (1 + 2)-body bound states in planar atomic waveguides. *Phys. Rev. A* **82**, 033625, DOI: [10.1103/PhysRevA.82.033625](https://doi.org/10.1103/PhysRevA.82.033625) (2010).

141. Ferlaino, F. *et al.* Evidence for universal four-body states tied to an Efimov trimer. *Phys. Rev. Lett.* **102**, 140401 (2009).

142. Bazak, B. & Petrov, D. S. Five-Body Efimov Effect and Universal Pentamer in Fermionic Mixtures. *Phys. Rev. Lett.* **118**, 083002, DOI: [10.1103/PhysRevLett.118.083002](https://doi.org/10.1103/PhysRevLett.118.083002) (2017).

143. Wenz, A. N. *et al.* From Few to Many: Observing the Formation of a Fermi Sea One Atom at a Time. *Science* **342**, 457–460, DOI: [10.1126/science.1240516](https://doi.org/10.1126/science.1240516) (2013). <https://www.science.org/doi/pdf/10.1126/science.1240516>.

144. Parish, M. M., Marchetti, F. M., Lamacraft, A. & Simons, B. D. Finite-temperature phase diagram of a polarized Fermi condensate. *Nat. Phys.* **3**, 124–128, DOI: [10.1038/nphys520](https://doi.org/10.1038/nphys520) (2007).

145. Landau, L. D. & Pekar, S. I. Effective mass of a polaron. *Zh. Eksp. Teor. Fiz.* **18**, 419–423 (1948).

146. Fröhlich, H. Electrons in lattice fields. *Adv. Phys.* **3**, 325–361, DOI: [10.1080/00018735400101213](https://doi.org/10.1080/00018735400101213) (1954).

147. Lan, Z. & Lobo, C. A single impurity in an ideal atomic Fermi gas: current understanding and some open problems. *J. Indian Inst. Sci.* **94**, DOI: [10.48550/ARXIV.1404.3220](https://doi.org/10.48550/ARXIV.1404.3220) (2014).

148. Grusdt, F. & Demler, E. New theoretical approaches to Bose polarons. In Inguscio, M., Ketterle, W., Stringari, S. & Roati, G. (eds.) *Quantum Matter at Ultralow Temperatures*, vol. 191 of *Proceedings of the International School of Physics "Enrico Fermi"*, 325–411, DOI: [10.3254/978-1-61499-694-1-325](https://doi.org/10.3254/978-1-61499-694-1-325) (IOS Press, 2016).

149. Scazza, F., Zaccanti, F., Massignan, P., Parish, M. M. & Jesper, J. Repulsive Fermi and Bose Polarons in Quantum Gases. *Atoms* **10**, 55, DOI: [10.3390/atoms10020055](https://doi.org/10.3390/atoms10020055) (2022).

150. Ness, G. *et al.* Observation of a Smooth Polaron-Molecule Transition in a Degenerate Fermi Gas. *Phys. Rev. X* **10**, 041019, DOI: [10.1103/PhysRevX.10.041019](https://doi.org/10.1103/PhysRevX.10.041019) (2020).

151. Nascimbène, S. *et al.* Collective Oscillations of an Imbalanced Fermi Gas: Axial Compression Modes and Polaron Effective Mass. *Phys. Rev. Lett.* **103**, 170402, DOI: [10.1103/PhysRevLett.103.170402](https://doi.org/10.1103/PhysRevLett.103.170402) (2009).

152. Levinsen, J., Parish, M. M. & Bruun, G. M. Impurity in a Bose-Einstein Condensate and the Efimov Effect. *Phys. Rev. Lett.* **115**, 125302, DOI: [10.1103/PhysRevLett.115.125302](https://doi.org/10.1103/PhysRevLett.115.125302) (2015).

153. Yan, Z. Z., Ni, Y., Robens, C. & Zwierlein, M. W. Bose polarons near quantum criticality. *Science* **368**, 6487, DOI: [10.1126/science.aax5850](https://doi.org/10.1126/science.aax5850) (2020).

154. Etrych, J. *et al.* Universal quantum dynamics of Bose polarons (2024). [2402.14816](https://doi.org/10.4249/2402.14816).

155. Mathy, C. J. M., Parish, M. M. & Huse, D. A. Trimers, Molecules, and Polarons in Mass-Imbalanced Atomic Fermi Gases. *Phys. Rev. Lett.* **106**, 166404, DOI: [10.1103/PhysRevLett.106.166404](https://doi.org/10.1103/PhysRevLett.106.166404) (2011).

156. Liu, R., Peng, C. & Cui, X. Emergence of crystalline few-body correlations in mass-imbalanced Fermi polarons. *Cell Reports Phys. Sci.* **3**, 100993, DOI: <https://doi.org/10.1016/j.xrpp.2022.100993> (2022).

157. Christianen, A., Cirac, J. I. & Schmidt, R. Bose polaron and the Efimov effect: A Gaussian-state approach. *Phys. Rev. A* **105**, 053302, DOI: [10.1103/PhysRevA.105.053302](https://doi.org/10.1103/PhysRevA.105.053302) (2022).

158. Goold, J., Fogarty, T., Lo Gullo, N., Paternostro, M. & Busch, T. Orthogonality catastrophe as a consequence of qubit embedding in an ultracold Fermi gas. *Phys. Rev. A* **84**, 063632, DOI: [10.1103/PhysRevA.84.063632](https://doi.org/10.1103/PhysRevA.84.063632) (2011).

159. Knap, M. *et al.* Time-dependent impurity in ultracold fermions: Orthogonality catastrophe and beyond. *Phys. Rev. X* **2**, 041020, DOI: [10.1103/PhysRevX.2.041020](https://doi.org/10.1103/PhysRevX.2.041020) (2012).

160. Anderson, P. W. Infrared Catastrophe in Fermi Gases with Local Scattering Potentials. *Phys. Rev. Lett.* **18**, 1049–1051, DOI: [10.1103/PhysRevLett.18.1049](https://doi.org/10.1103/PhysRevLett.18.1049) (1967).

161. Guenther, N.-E., Schmidt, R., Bruun, G. M., Gurarie, V. & Massignan, P. Mobile impurity in a Bose-Einstein condensate and the orthogonality catastrophe. *Phys. Rev. A* **103**, 013317, DOI: [10.1103/PhysRevA.103.013317](https://doi.org/10.1103/PhysRevA.103.013317) (2021).

162. Vale, C. J. & Zwierlein, M. Spectroscopic probes of quantum gases. *Nat. Phys.* **17**, 1305–1315, DOI: [10.1038/s41567-021-01434-6](https://doi.org/10.1038/s41567-021-01434-6) (2021).

163. Kohstall, C. *et al.* Metastability and coherence of repulsive polarons in a strongly interacting Fermi mixture. *Nat. (London)* **485**, 615–618, DOI: [10.1038/nature11065](https://doi.org/10.1038/nature11065) (2012).

164. Fritzsche, I. *et al.* Stability and breakdown of Fermi polarons in a strongly interacting Fermi-Bose mixture. *Phys. Rev. A* **103**, 053314, DOI: [10.1103/PhysRevA.103.053314](https://doi.org/10.1103/PhysRevA.103.053314) (2021).

165. Hu, M.-G. *et al.* Bose polarons in the strongly interacting regime. *Phys. Rev. Lett.* **117**, 055301, DOI: [10.1103/PhysRevLett.117.055301](https://doi.org/10.1103/PhysRevLett.117.055301) (2016).

166. Jørgensen, N. B. *et al.* Observation of Attractive and Repulsive Polarons in a Bose-Einstein Condensate. *Phys. Rev. Lett.* **117**, 055302, DOI: [10.1103/PhysRevLett.117.055302](https://doi.org/10.1103/PhysRevLett.117.055302) (2016).

167. Cetina, M. *et al.* Ultrafast many-body interferometry of impurities coupled to a Fermi sea. *Science* **354**, 96–99, DOI: [10.1126/science.aaf5134](https://doi.org/10.1126/science.aaf5134) (2016).

168. Skou, M. G. *et al.* Non-equilibrium quantum dynamics and formation of the Bose polaron. *Nat. Phys.* 731–735, DOI: [10.1038/s41567-021-01184-5](https://doi.org/10.1038/s41567-021-01184-5) (2021).

169. Adlong, H. S. *et al.* Quasiparticle Lifetime of the Repulsive Fermi Polaron. *Phys. Rev. Lett.* **125**, 133401, DOI: [10.1103/PhysRevLett.125.133401](https://doi.org/10.1103/PhysRevLett.125.133401) (2020).

170. Chikkatur, A. P. *et al.* Suppression and Enhancement of Impurity Scattering in a Bose-Einstein Condensate. *Phys. Rev. Lett.* **85**, 483–486, DOI: [10.1103/PhysRevLett.85.483](https://doi.org/10.1103/PhysRevLett.85.483) (2000).

171. Koschorreck, M. *et al.* Attractive and repulsive Fermi polarons in two dimensions. *Nat. (Lon)* **485**, 619–622 (2012).

172. Yu, Z. & Pethick, C. J. Induced interactions in dilute atomic gases and liquid helium mixtures. *Phys. Rev. A* **85**, 063616, DOI: [10.1103/PhysRevA.85.063616](https://doi.org/10.1103/PhysRevA.85.063616) (2012).

173. Baroni, C. *et al.* Mediated interactions between Fermi polarons and the role of impurity quantum statistics. *Nat. Phys.* **20**, 68–73, DOI: <https://doi.org/10.1038/s41567-023-02248-4> (2024).

174. Camacho-Guardian, A., Peña Ardila, L. A., Pohl, T. & Bruun, G. M. Bipolarons in a Bose-Einstein Condensate. *Phys. Rev. Lett.* **121**, 013401, DOI: [10.1103/PhysRevLett.121.013401](https://doi.org/10.1103/PhysRevLett.121.013401) (2018).

175. Mistakidis, S. & Volosniev, A. Physics of impurities in quantum gases. *Atoms* DOI: <https://doi.org/10.3390/books978-3-0365-4874-6> (2022).

176. Palzer, S., Zipkes, C., Sias, C. & Köhl, M. Quantum Transport through a Tonks-Girardeau Gas. *Phys. Rev. Lett.* **103**, 150601, DOI: [10.1103/PhysRevLett.103.150601](https://doi.org/10.1103/PhysRevLett.103.150601) (2009).

177. Catani, J. *et al.* Quantum dynamics of impurities in a one-dimensional Bose gas. *Phys. Rev. A* **85**, 023623, DOI: [10.1103/PhysRevA.85.023623](https://doi.org/10.1103/PhysRevA.85.023623) (2012).

178. Meinert, F. *et al.* Bloch oscillations in the absence of a lattice. *Science* **356**, 945–948, DOI: [10.1126/science.aaah6616](https://doi.org/10.1126/science.aaah6616) (2017). <https://www.science.org/doi/pdf/10.1126/science.aaah6616>.

179. Pérez-Ríos, J. Cold chemistry: a few-body perspective on impurity physics of a single ion in an ultracold bath. *Mol. Phys.* **119**, e1881637, DOI: [10.1080/00268976.2021.1881637](https://doi.org/10.1080/00268976.2021.1881637) (2021).

180. Zipkes, C., Palzer, S., Sias, C. & Köhl, M. A trapped single ion inside a Bose-Einstein condensate. *Nature* **464**, 388–391, DOI: [10.1038/nature08865](https://doi.org/10.1038/nature08865) (2010).

181. Camargo, F. *et al.* Creation of Rydberg Polarons in a Bose Gas. *Phys. Rev. Lett.* **120**, 083401, DOI: [10.1103/PhysRevLett.120.083401](https://doi.org/10.1103/PhysRevLett.120.083401) (2018).

182. Hu, H., Drummond, P. D. & Liu, X.-J. Universal thermodynamics of strongly interacting Fermi gases. *Nat. Phys.* **3**, 469–472, DOI: [10.1038/nphys598](https://doi.org/10.1038/nphys598) (2007).

183. Jochim, S. *et al.* Bose-Einstein Condensation of Molecules. *Science* **302**, 2101–2103, DOI: [10.1126/science.1093280](https://doi.org/10.1126/science.1093280) (2003).

184. Zwierlein, M. W. *et al.* Observation of Bose-Einstein Condensation of Molecules. *Phys. Rev. Lett.* **91**, 250401, DOI: [10.1103/PhysRevLett.91.250401](https://doi.org/10.1103/PhysRevLett.91.250401) (2003).

185. Greiner, M., Regal, C. A. & Jin, D. S. Emergence of a Molecular Bose-Einstein Condensate from a Fermi Gas. *Nat. (London)* **426**, 537–540, DOI: [doi.org/10.1038/nature02199](https://doi.org/10.1038/nature02199) (2003).

186. Regal, C. A., Ticknor, C., Bohn, J. L. & Jin, D. S. Creation of ultracold molecules from a Fermi gas of atoms. *Nat. (London)* **424**, 47–50, DOI: [10.1038/nature01738](https://doi.org/10.1038/nature01738) (2003).

187. Bardeen, J., Cooper, L. N. & Schrieffer, J. R. Theory of superconductivity. *Phys. Rev.* **108**, 1175–1204 (1957).

188. Cooper, L. N. Bound Electron Pairs in a Degenerate Fermi Gas. *Phys. Rev.* **104**, 1189–1190, DOI: [10.1103/PhysRev.104.1189](https://doi.org/10.1103/PhysRev.104.1189) (1956).

189. Holten, M. *et al.* Observation of Cooper pairs in a mesoscopic two-dimensional Fermi gas. *Nature* **606**, 287–291, DOI: [10.1038/s41586-022-04678-1](https://doi.org/10.1038/s41586-022-04678-1) (2022).

190. Regal, C. A., Greiner, M. & Jin, D. S. Observation of resonance condensation of fermionic atom pairs. *Phys. Rev. Lett.* **92**, 040403, DOI: [10.1103/PhysRevLett.92.040403](https://doi.org/10.1103/PhysRevLett.92.040403) (2004).

191. Kinast, J., Hemmer, S. L., Gehm, M. E., Turlapov, A. & Thomas, J. E. Evidence for Superfluidity in a Resonantly Interacting Fermi Gas. *Phys. Rev. Lett.* **92**, 150402, DOI: [10.1103/PhysRevLett.92.150402](https://doi.org/10.1103/PhysRevLett.92.150402) (2004).

192. Bartenstein, M. *et al.* Collective Excitations of a Degenerate Gas at the BEC-BCS Crossover. *Phys. Rev. Lett.* **92**, 203201, DOI: [10.1103/PhysRevLett.92.203201](https://doi.org/10.1103/PhysRevLett.92.203201) (2004).

193. Bourdel, T. *et al.* Experimental study of the bec-bcs crossover region in lithium 6. *Phys. Rev. Lett.* **93**, 050401 (2004).

194. Zwierlein, M. W., Abo-Shaeer, J. R., Schirotzek, A., Schunck, C. H. & Ketterle, W. Vortices and Superfluidity in a Strongly Interacting Fermi Gas. *Nat. (London)* **435**, 1047–1051, DOI: [10.1038/nature03858](https://doi.org/10.1038/nature03858) (2005).

195. Grimm, R. Ultracold Fermi gases in the BEC-BCS crossover: A review from the Innsbruck perspective. *Proc. Int. Sch. Phys. "Enrico Fermi"* **164**, 413–462, DOI: [10.3254/978-1-58603-846-5-413](https://doi.org/10.3254/978-1-58603-846-5-413) (2007).

196. Randeria, M. & Taylor, E. Crossover from Bardeen-Cooper-Schrieffer to Bose-Einstein Condensation and the Unitary Fermi Gas. *Annu. Rev. Condens. Matter Phys.* **5**, 209–232, DOI: <https://doi.org/10.1146/annurev-conmatphys-031113-133829> (2014).

197. Lobo, C., Recati, A., Giorgini, S. & Stringari, S. Normal State of a Polarized Fermi Gas at Unitarity. *Phys. Rev. Lett.* **97**, 200403, DOI: [10.1103/PhysRevLett.97.200403](https://doi.org/10.1103/PhysRevLett.97.200403) (2006).

198. Chandrasekhar, B. S. A note on the maximum critical field of high-field superconductors. *Appl. Phys. Lett.* **1**, 7–8, DOI: [10.1063/1.1777362](https://doi.org/10.1063/1.1777362) (1962). <https://doi.org/10.1063/1.1777362>.

199. Clogston, A. M. Upper Limit for the Critical Field in Hard Superconductors. *Phys. Rev. Lett.* **9**, 266–267, DOI: [10.1103/PhysRevLett.9.266](https://doi.org/10.1103/PhysRevLett.9.266) (1962).

200. Zwierlein, M. W., Schirotzek, A., Schunck, C. H. & Ketterle, W. Fermionic Superfluidity with Imbalanced Spin Populations. *Science* **311**, 492–496, DOI: [10.1126/science.1122318](https://doi.org/10.1126/science.1122318) (2006).

201. Zwierlein, M. W., Schirotzek, A., Schunck, C. H. & Ketterle, W. Direct observation of the superfluid phase transition in ultracold Fermi gases. *Nat. (London)* **442**, 54–58, DOI: [doi:10.1038/nature04936](https://doi.org/10.1038/nature04936) (2006).

202. Partridge, G. B., Li, W., Kamar, R. I., Liao, Y. & Hulet, R. G. Pairing and Phase Separation in a Polarized Fermi Gas. *Science* **311**, 503–505 (2006).

203. Gubbels, K. B. & Stoof, H. T. C. Imbalanced Fermi gases at unitarity. *Phys. Rep.* **525**, 255 – 313, DOI: [10.1016/j.physrep.2012.11.004](https://doi.org/10.1016/j.physrep.2012.11.004) (2013).

204. Combescot, R. Introduction to FFLO phases and collective mode in the BEC-BCS crossover. *Proc. Int. Sch. Phys. "Enrico Fermi"* **164**, 697–714, DOI: [10.3254/978-1-58603-846-5-697](https://doi.org/10.3254/978-1-58603-846-5-697) (2007).

205. Kinnunen, J. J., Baarsma, J. E., Martikainen, J.-P. & Törmä, P. The Fulde–Ferrell–Larkin–Ovchinnikov state for ultracold fermions in lattice and harmonic potentials: a review. *Reports on Prog. Phys.* **81**, 046401, DOI: [10.1088/1361-6633/aaa4ad](https://doi.org/10.1088/1361-6633/aaa4ad) (2018).

206. Pini, M., Pieri, P. & Calvanese Strinati, G. Evolution of an attractive polarized Fermi gas: From a Fermi liquid of polarons to a non-Fermi liquid at the Fulde-Ferrell-Larkin-Ovchinnikov quantum critical point. *Phys. Rev. B* **107**, 054505, DOI: [10.1103/PhysRevB.107.054505](https://doi.org/10.1103/PhysRevB.107.054505) (2023).

207. Sarma, G. On the influence of a uniform exchange field acting on the spins of the conduction electrons in a superconductor. *J. Phys. Chem. Solids* **24**, 1029–1032, DOI: [10.1016/0022-3697\(63\)90007-6](https://doi.org/10.1016/0022-3697(63)90007-6) (1963).

208. Gubbels, K. B., Romans, M. W. J. & Stoof, H. T. C. Sarma Phase in Trapped Unbalanced Fermi Gases. *Phys. Rev. Lett.* **97**, 210402, DOI: [10.1103/PhysRevLett.97.210402](https://doi.org/10.1103/PhysRevLett.97.210402) (2006).

209. Pini, M., Pieri, P., Grimm, R. & Strinati, G. C. Beyond-mean-field description of a trapped unitary Fermi gas with mass and population imbalance. *Phys. Rev. A* **103**, 023314, DOI: [10.1103/PhysRevA.103.023314](https://doi.org/10.1103/PhysRevA.103.023314) (2021).

210. Voigt, A.-C. *et al.* Ultracold Heteronuclear Fermi-Fermi Molecules. *Phys. Rev. Lett.* **102**, 020405, DOI: [10.1103/PhysRevLett.102.020405](https://doi.org/10.1103/PhysRevLett.102.020405) (2009). *ibid.* **105**, 269904(E) (2010).

211. Hara, H., Takasu, Y., Yamaoka, Y., Doyle, J. M. & Takahashi, Y. Quantum Degenerate Mixtures of Alkali and Alkaline-Earth-Like Atoms. *Phys. Rev. Lett.* **106**, 205304, DOI: [10.1103/PhysRevLett.106.205304](https://doi.org/10.1103/PhysRevLett.106.205304) (2011).

212. Schäfer, F., Haruna, Y. & Takahashi, Y. Observation of Feshbach Resonances in an  $^{167}\text{Er}$ – $^6\text{Li}$  Fermi–Fermi Mixture. *J. Phys. Soc. Jpn.* **92**, 054301, DOI: [10.7566/JPSJ.92.054301](https://doi.org/10.7566/JPSJ.92.054301) (2023). <https://doi.org/10.7566/JPSJ.92.054301>.

213. Dagotto, E. Complexity in strongly correlated electronic systems. *Science* **309**, 257–262 (2005).

214. Dagotto, E., Burgoy, J. & Moreo, A. Nanoscale phase separation in colossal magnetoresistance materials: lessons for the cuprates? *Solid State Commun.* **126**, 9–22 (2003).

215. Cui, X. & Ho, T.-L. Phase Separation in Mixtures of Repulsive Fermi Gases Driven by Mass Difference. *Phys. Rev. Lett.* **110**, 165302, DOI: [10.1103/PhysRevLett.110.165302](https://doi.org/10.1103/PhysRevLett.110.165302) (2013).

216. Ho, T.-L. & Shenoy, V. B. Binary Mixtures of Bose Condensates of Alkali Atoms. *Phys. Rev. Lett.* **77**, 3276–3279, DOI: [10.1103/PhysRevLett.77.3276](https://doi.org/10.1103/PhysRevLett.77.3276) (1996).

217. Makotyn, P., Klauss, C. E., Goldberger, D. L., Cornell, E. A. & Jin, D. S. Universal dynamics of a degenerate unitary Bose gas. *Nat. Phys.* **10**, 116–119, DOI: [10.1038/nphys2850](https://doi.org/10.1038/nphys2850) (2014).

218. Eigen, C. *et al.* Universal prethermal dynamics of Bose gases quenched to unitarity. *Nature* **563**, 221–224, DOI: [10.1038/s41586-018-0674-1](https://doi.org/10.1038/s41586-018-0674-1) (2018).

219. Bienaimé, T. *et al.* Spin-dipole oscillation and polarizability of a binary Bose-Einstein condensate near the miscible-immiscible phase transition. *Phys. Rev. A* **94**, 063652, DOI: [10.1103/PhysRevA.94.063652](https://doi.org/10.1103/PhysRevA.94.063652) (2016).

220. Kim, J. H., Hong, D. & Shin, Y. Observation of two sound modes in a binary superfluid gas. *Phys. Rev. A* **101**, 061601, DOI: [10.1103/PhysRevA.101.061601](https://doi.org/10.1103/PhysRevA.101.061601) (2020).

221. Cominotti, R. *et al.* Observation of Massless and Massive Collective Excitations with Faraday Patterns in a Two-Component Superfluid. *Phys. Rev. Lett.* **128**, 210401, DOI: [10.1103/PhysRevLett.128.210401](https://doi.org/10.1103/PhysRevLett.128.210401) (2022).

222. Cavicchioli, L., Fort, C., Modugno, M., Minardi, F. & Burchianti, A. Dipole dynamics of an interacting bosonic mixture. *Phys. Rev. Res.* **4**, 043068, DOI: [10.1103/PhysRevResearch.4.043068](https://doi.org/10.1103/PhysRevResearch.4.043068) (2022).

223. Kim, J. H., Seo, S. W. & Shin, Y. Critical Spin Superflow in a Spinor Bose-Einstein Condensate. *Phys. Rev. Lett.* **119**, 185302, DOI: [10.1103/PhysRevLett.119.185302](https://doi.org/10.1103/PhysRevLett.119.185302) (2017).

224. Pyzh, M. & Schmelcher, P. Phase separation of a Bose-Bose mixture: Impact of the trap and particle-number imbalance. *Phys. Rev. A* **102**, 023305, DOI: [10.1103/PhysRevA.102.023305](https://doi.org/10.1103/PhysRevA.102.023305) (2020).

225. Naidon, P. & Petrov, D. S. Mixed Bubbles in Bose-Bose Mixtures. *Phys. Rev. Lett.* **126**, 115301, DOI: [10.1103/PhysRevLett.126.115301](https://doi.org/10.1103/PhysRevLett.126.115301) (2021).

226. Yi, S., Müstecaplıoğlu, O. E., Sun, C. P. & You, L. Single-mode approximation in a spinor-1 atomic condensate. *Phys. Rev. A* **66**, 011601, DOI: [10.1103/PhysRevA.66.011601](https://doi.org/10.1103/PhysRevA.66.011601) (2002).

227. Frapolli, C. *et al.* Stepwise Bose-Einstein Condensation in a Spinor Gas. *Phys. Rev. Lett.* **119**, 050404, DOI: [10.1103/PhysRevLett.119.050404](https://doi.org/10.1103/PhysRevLett.119.050404) (2017).

228. Kevrekidis, P. G., Nistazakis, H. E., Frantzeskakis, D. J., Malomed, B. A. & Carretero-González, R. Families of matter-waves in two-component Bose-Einstein condensates. *Eur. Phys. J. D* **28**, 181–185, DOI: [10.1140/epjd/e2003-00311-6](https://doi.org/10.1140/epjd/e2003-00311-6) (2004).

229. Bakkali-Hassani, B. *et al.* Realization of a Townes Soliton in a Two-Component Planar Bose Gas. *Phys. Rev. Lett.* **127**, 023603, DOI: [10.1103/PhysRevLett.127.023603](https://doi.org/10.1103/PhysRevLett.127.023603) (2021).

230. Romero-Ros, A. *et al.* Experimental Realization of the Peregrine Soliton in Repulsive Two-Component Bose-Einstein Condensates. *Phys. Rev. Lett.* **132**, 033402, DOI: [10.1103/PhysRevLett.132.033402](https://doi.org/10.1103/PhysRevLett.132.033402) (2024).

231. Hamner, C., Chang, J. J., Engels, P. & Hoefer, M. A. Generation of dark-bright soliton trains in superfluid-superfluid counterflow. *Phys. Rev. Lett.* **106**, 065302, DOI: [10.1103/PhysRevLett.106.065302](https://doi.org/10.1103/PhysRevLett.106.065302) (2011).

232. Farolfi, A., Trypogeorgos, D., Mordini, C., Lamporesi, G. & Ferrari, G. Observation of Magnetic Solitons in Two-Component Bose-Einstein Condensates. *Phys. Rev. Lett.* **125**, 030401, DOI: [10.1103/PhysRevLett.125.030401](https://doi.org/10.1103/PhysRevLett.125.030401) (2020).

233. Chai, X. *et al.* Magnetic Solitons in a Spin-1 Bose-Einstein Condensate. *Phys. Rev. Lett.* **125**, 030402, DOI: [10.1103/PhysRevLett.125.030402](https://doi.org/10.1103/PhysRevLett.125.030402) (2020).

234. Seo, S. W., Kang, S., Kwon, W. J. & Shin, Y.-i. Half-Quantum Vortices in an Antiferromagnetic Spinor Bose-Einstein Condensate. *Phys. Rev. Lett.* **115**, 015301, DOI: [10.1103/PhysRevLett.115.015301](https://doi.org/10.1103/PhysRevLett.115.015301) (2015).

235. Richaud, A., Lamporesi, G., Capone, M. & Recati, A. Mass-driven vortex collisions in flat superfluids. *Phys. Rev. A* **107**, 053317, DOI: [10.1103/PhysRevA.107.053317](https://doi.org/10.1103/PhysRevA.107.053317) (2023).

236. Farolfi, A. *et al.* Quantum-torque-induced breaking of magnetic interfaces in ultracold gases. *Nat. Phys.* **17**, 1359–1363 (2021).

237. Eto, M. & Nitta, M. Confinement of half-quantized vortices in coherently coupled Bose-Einstein condensates: Simulating quark confinement in a QCD-like theory. *Phys. Rev. A* **97**, 023613, DOI: [10.1103/PhysRevA.97.023613](https://doi.org/10.1103/PhysRevA.97.023613) (2018).

238. Zenesini, A. *et al.* False vacuum decay via bubble formation in ferromagnetic superfluids. *Nat. Phys.* DOI: [10.1038/s41567-023-02345-4](https://doi.org/10.1038/s41567-023-02345-4) (2024).

239. Tolosa-Simeón, M. *et al.* Curved and expanding spacetime geometries in Bose-Einstein condensates. *Phys. Rev. A* **106**, 033313, DOI: [10.1103/PhysRevA.106.033313](https://doi.org/10.1103/PhysRevA.106.033313) (2022).

240. Lin, Y.-J., Compton, R. L., Jimenez-Garcia, K., Porto, J. V. & Spielman, I. B. Synthetic magnetic fields for ultracold neutral atoms. *Nat. (London)* **462**, 628–632, DOI: [10.1038/nature08609](https://doi.org/10.1038/nature08609) (2009).

241. Putra, A., Salces-Cárcoba, F., Yue, Y., Sugawa, S. & Spielman, I. B. Spatial Coherence of Spin-Orbit-Coupled Bose Gases. *Phys. Rev. Lett.* **124**, 053605, DOI: [10.1103/PhysRevLett.124.053605](https://doi.org/10.1103/PhysRevLett.124.053605) (2020).

242. Roati, G., Riboli, F., Modugno, G. & Inguscio, M. Fermi-Bose Quantum Degenerate K-Rb Mixture with Attractive Interaction. *Phys. Rev. Lett.* **89**, 150403, DOI: [10.1103/PhysRevLett.89.150403](https://doi.org/10.1103/PhysRevLett.89.150403) (2002).

243. Goldwin, J. *et al.* Measurement of the interaction strength in a Bose-Fermi mixture with  $^{87}\text{Rb}$  and  $^{40}\text{K}$ . *Phys. Rev. A* **70**, 021601, DOI: [10.1103/PhysRevA.70.021601](https://doi.org/10.1103/PhysRevA.70.021601) (2004).

244. Köhl, M., Moritz, H., Stöferle, T., Günter, K. & Esslinger, T. Fermionic Atoms in a Three Dimensional Optical Lattice: Observing Fermi Surfaces, Dynamics, and Interactions. *Phys. Rev. Lett.* **94**, 080403 (2005).

245. Hadzibabic, Z. *et al.* Fiftyfold improvement in the number of quantum degenerate fermionic atoms. *Phys. Rev. Lett.* **91**, 160401 (2003).

246. Ferrier-Barbut, I. *et al.* A mixture of Bose and Fermi superfluids. *Science* **345**, 1035–1038, DOI: [10.1126/science.1255380](https://doi.org/10.1126/science.1255380) (2014).

247. Viverit, L., Pethick, C. J. & Smith, H. Zero-temperature phase diagram of binary boson-fermion mixtures. *Phys. Rev. A* **61**, 053605, DOI: [10.1103/PhysRevA.61.053605](https://doi.org/10.1103/PhysRevA.61.053605) (2000).

248. Modugno, G. Fermi-Bose mixture with tunable interactions. *Proc. Int. Sch. Phys. "Enrico Fermi"* **164**, 657–675, DOI: [10.3254/978-1-58603-846-5-657](https://doi.org/10.3254/978-1-58603-846-5-657) (2007).

249. Lous, R. S. *et al.* Probing the Interface of a Phase-Separated State in a Repulsive Bose-Fermi Mixture. *Phys. Rev. Lett.* **120**, 243403, DOI: [10.1103/PhysRevLett.120.243403](https://doi.org/10.1103/PhysRevLett.120.243403) (2018).

250. Efremov, D. V. & Viverit, L.  $p$ -wave cooper pairing of fermions in mixtures of dilute fermi and bose gases. *Phys. Rev. B* **65**, 134519, DOI: [10.1103/PhysRevB.65.134519](https://doi.org/10.1103/PhysRevB.65.134519) (2002).

251. Kinnunen, J. J., Wu, Z. & Bruun, G. M. Induced  $p$ -Wave Pairing in Bose-Fermi Mixtures. *Phys. Rev. Lett.* **121**, 253402, DOI: [10.1103/PhysRevLett.121.253402](https://doi.org/10.1103/PhysRevLett.121.253402) (2018).

252. DeSalvo, B., Patel, K., Cai, G. & Cheng, C. Observation of fermion-mediated interactions between bosonic atoms. *Nature* **568**, 61–64, DOI: <https://doi.org/10.1038/s41586-019-1055-0> (2019).

253. Edri, H., Raz, B., Matzliah, N., Davidson, N. & Ozeri, R. Observation of Spin-Spin Fermion-Mediated Interactions between Ultracold Bosons. *Phys. Rev. Lett.* **124**, 163401, DOI: [10.1103/PhysRevLett.124.163401](https://doi.org/10.1103/PhysRevLett.124.163401) (2020).

254. Argüello-Luengo, J., González-Tudela, A. & González-Cuadra, D. Tuning Long-Range Fermion-Mediated Interactions in Cold-Atom Quantum Simulators. *Phys. Rev. Lett.* **129**, 083401, DOI: [10.1103/PhysRevLett.129.083401](https://doi.org/10.1103/PhysRevLett.129.083401) (2022).

255. Cazalilla, M. A., Citro, R., Giamarchi, T., Orignac, E. & Rigol, M. One dimensional bosons: From condensed matter systems to ultracold gases. *Rev. Mod. Phys.* **83**, 1405–1466, DOI: [10.1103/RevModPhys.83.1405](https://doi.org/10.1103/RevModPhys.83.1405) (2011).

256. Mistakidis, S. *et al.* Few-body bose gases in low dimensions—a laboratory for quantum dynamics. *Phys. Reports* **1042**, 1–108, DOI: <https://doi.org/10.1016/j.physrep.2023.10.004> (2023). Few-body Bose gases in low dimensions—A laboratory for quantum dynamics.

257. Ozawa, T. & Price, H. M. Topological quantum matter in synthetic dimensions. *Nat. Rev. Phys.* **1**, 349–357, DOI: [10.1038/s42254-019-0045-3](https://doi.org/10.1038/s42254-019-0045-3) (2019).

258. Fabre, A. & Nascimbene, S. Atomic topological quantum matter using synthetic dimensions. *Europhys. Lett.* **145**, 65001, DOI: [10.1209/0295-5075/ad2ff6](https://doi.org/10.1209/0295-5075/ad2ff6) (2024).

259. Cui, Y., Deng, M., You, L., Gao, B. & Tey, M. K. Broad Feshbach resonances in ultracold alkali-metal systems. *Phys. Rev. A* **98**, 042708, DOI: [10.1103/PhysRevA.98.042708](https://doi.org/10.1103/PhysRevA.98.042708) (2018).

260. Chomaz, L. *et al.* Dipolar physics: a review of experiments with magnetic quantum gases. *Reports on Prog. Phys.* **86**, 026401, DOI: [10.1088/1361-6633/aca814](https://doi.org/10.1088/1361-6633/aca814) (2022).

261. Weckesser, P. *et al.* Observation of Feshbach resonances between a single ion and ultracold atoms. *Nature* **600**, 429–433, DOI: [10.1038/s41586-021-04112-y](https://doi.org/10.1038/s41586-021-04112-y) (2021).

262. Fischer, U. R. & Schützhold, R. Quantum simulation of cosmic inflation in two-component Bose-Einstein condensates. *Phys. Rev. A* **70**, 063615, DOI: [10.1103/PhysRevA.70.063615](https://doi.org/10.1103/PhysRevA.70.063615) (2004).

263. Visser, M. & Weinfurtner, S. Massive Klein-Gordon equation from a Bose-Einstein-condensation-based analogue spacetime. *Phys. Rev. D* **72**, 044020, DOI: [10.1103/PhysRevD.72.044020](https://doi.org/10.1103/PhysRevD.72.044020) (2005).

264. Liberati, S., Visser, M. & Weinfurtner, S. Analogue quantum gravity phenomenology from a two-component Bose–Einstein condensate. *Class. Quantum Gravity* **23**, 3129, DOI: [10.1088/0264-9381/23/9/023](https://doi.org/10.1088/0264-9381/23/9/023) (2006).

265. Butera, S., Öhberg, P. & Carusotto, I. Black-hole lasing in coherently coupled two-component atomic condensates. *Phys. Rev. A* **96**, 013611, DOI: [10.1103/PhysRevA.96.013611](https://doi.org/10.1103/PhysRevA.96.013611) (2017).

266. Amico, L. *et al.* Colloquium: Atomtronic circuits: From many-body physics to quantum technologies. *Rev. Mod. Phys.* **94**, 041001, DOI: [10.1103/RevModPhys.94.041001](https://doi.org/10.1103/RevModPhys.94.041001) (2022).

267. Nishida, Y. & Tan, S. Universal Fermi gases in mixed dimensions. *Phys. Rev. Lett.* **101**, 170401 (2008).

268. Nishida, Y. & Tan, S. Confinement-induced Efimov resonances in Fermi-Fermi mixtures. *Phys. Rev. A* **79**, 060701(R), DOI: [10.1103/PhysRevA.79.060701](https://doi.org/10.1103/PhysRevA.79.060701) (2009).

269. Caracanhas, M. A., Schreck, F. & Smith, C. M. Fermi-Bose mixture in mixed dimensions. *New J. Phys.* **19**, 115011, DOI: [10.1088/1367-2630/aa8e56](https://doi.org/10.1088/1367-2630/aa8e56) (2017).

270. Schäfer, F. *et al.* Experimental realization of ultracold Yb-<sup>7</sup>Li mixtures in mixed dimensions. *Phys. Rev. A* **98**, 051602, DOI: [10.1103/PhysRevA.98.051602](https://doi.org/10.1103/PhysRevA.98.051602) (2018).

271. Ravensbergen, C. *et al.* Accurate Determination of the Dynamical Polarizability of Dysprosium. *Phys. Rev. Lett.* **120**, 223001, DOI: [10.1103/PhysRevLett.120.223001](https://doi.org/10.1103/PhysRevLett.120.223001) (2018).

272. Wang, J., Che, Y., Zhang, L. & Chen, Q. Enhancement effect of mass imbalance on Fulde-Ferrell-Larkin-Ovchinnikov type of pairing in Fermi-Fermi mixtures of ultracold quantum gases. *Sci. Rep.* **7**, 39783, DOI: [10.1038/srep39783](https://doi.org/10.1038/srep39783) (2017).

273. Liu, R., Peng, C. & Cui, X. Universal Tetramer and Pentamer Bound States in Two-Dimensional Fermionic Mixtures. *Phys. Rev. Lett.* **129**, 073401, DOI: [10.1103/PhysRevLett.129.073401](https://doi.org/10.1103/PhysRevLett.129.073401) (2022).